

UNCLASSIFIED

AD NUMBER
AD878415
NEW LIMITATION CHANGE
TO Approved for public release, distribution unlimited
FROM Distribution authorized to U.S. Gov't. agencies and their contractors; Administrative/Operational Use; OCT 1970. Other requests shall be referred to Air Force Flight Dynamics Lab., Wright-Patterson AFB, OH 45433.
AUTHORITY
AFFDL ltr, 25 Oct 1972

THIS PAGE IS UNCLASSIFIED

AD878415

AFFDL-TR-70-101

**HIGH ALTITUDE GUST CRITERIA  
FOR AIRCRAFT DESIGN**



*EDWARD V. ASHBURN, DAVID E. WACO AND CRAIG A. MELVIN  
LOCKHEED-CALIFORNIA COMPANY*

AD No. \_\_\_\_\_  
PFC FILE COPY

TECHNICAL REPORT AFFDL-TR-70-101

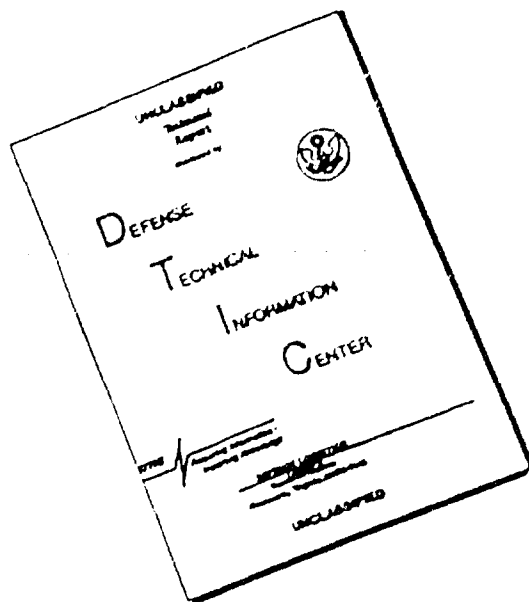
OCTOBER 1970

DDC  
RECEIVED  
JAN 11 1971  
RECEIVED  
B

This document is subject to special export controls and each transmittal to foreign governments or foreign nationals may be made only with prior approval of the Air Force Flight Dynamics Laboratory (FDTE), Wright-Patterson AFB, Ohio 45433.

AIR FORCE FLIGHT DYNAMICS LABORATORY  
AIR FORCE SYSTEMS COMMAND  
WRIGHT-PATTERSON AIR FORCE BASE, OHIO

# DISCLAIMER NOTICE



THIS DOCUMENT IS BEST QUALITY AVAILABLE. THE COPY FURNISHED TO DTIC CONTAINED A SIGNIFICANT NUMBER OF PAGES WHICH DO NOT REPRODUCE LEGIBLY.

NOTICE

When Government drawings, specifications, or other data are used for any purpose other than in connection with a definitely related Government procurement operation, the United States Government thereby incurs no responsibility nor any obligation whatsoever; and the fact that the government may have formulated, furnished, or in any way supplied the said drawings, specifications, or other data, is not to be regarded by implication or otherwise as in any manner licensing the holder or any other person or corporation, or conveying any rights or permission to manufacture, use, or sell any patented invention that may in any way be related thereto.

ACCESSION		
WPTI		
DOC	REF SECTION	<input checked="" type="checkbox"/>
UNCLASSIFIED		<input type="checkbox"/>
DISSECTION		
BY		
DISTRIBUTION AVAILABILITY CODES		
DIST.	AVAIL.	CODE OR SPECIAL
2		

Copies of this report should not be returned unless return is required by security considerations, contractual obligations, or notice on a specific document.

**AFFDL-TR-70-101**

**HIGH ALTITUDE GUST CRITERIA  
FOR AIRCRAFT DESIGN**

*EDWARD V. ASHBURN, DAVID E. WACO AND CRAIG A. MELVIN*

This document is subject to special export controls and each transmittal to foreign governments or foreign nationals may be made only with prior approval of the Air Force Flight Dynamics Laboratory (FDTE), Wright-Patterson AFB, Ohio 45433.

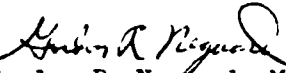
## FOREWORD

This report was prepared by the Lockheed-California Company, Burbank, California for the Air Force Flight Dynamics Laboratory, Wright-Patterson Air Force Base, Ohio under Contract F33615-69-C-1552. The contract title was "Development of High Altitude Gust Criteria for Aircraft Design". The contract was initiated under Advanced Development Program 682E, HICAT Project 682E-06. The Lockheed-California Company report number is LR-23670. The report covers work conducted from 17 March 1969 to 16 September 1970.

The contract was administered by the Air Force Flight Dynamics Laboratory, Wright-Patterson Air Force Base, Ohio, with Mr. Paul L. Hasty (FDTE) as Project Engineer. The Lockheed-California Company Principal Investigator was Edward V. Ashburn. Special acknowledgements are due to Dr. Arnold Court, Consultant for the program and to the following Lockheed-California Company personnel: Dr. D. T. Perkins, Division Scientist, Physical and Life Sciences Laboratory; Mr. D. T. Prophet, Mr. W. M. Crooks, Mr. F. A. Mitchell, Dr. S. I. Adelfang, Mr. J. E. Wignot, Mr. F. M. Hoblit, and Mr. Raphael Ortasse.

This report was submitted by the authors in September 1970.

This technical report has been reviewed and is approved.

  
Gordon R. Negard, Major, USAF  
Chief, Design Criteria Branch  
Structures Division

## ABSTRACT

Analysis of data obtained during the High Altitude Clear Air Turbulence Program in the altitude range 45,000 to 70,000 ft. indicated that probability densities and exceedances of root-mean-square (RMS) gust velocities varied significantly with the character of underlying topography and to a lesser degree with altitude. The relative frequency of occurrence of large RMS values increased with terrain roughness. The components of the RMS gust velocities were linearly related, with the lateral and longitudinal component values being larger than the vertical.

Lengths of the turbulent regions ranged from less than one mile to 130 miles, with the frequency of occurrence decreasing rapidly with increasing length. Because the long regions were small in number, relatively few power spectral density curves were derived over the frequency range necessary in computing scale lengths. Large scale lengths (generally 8,000 to 16,000 ft) and relatively steep slopes (-1.5 to -1.7) were suggested for mountain-related cases and for the lateral and longitudinal components from the few spectra available. Scale lengths were equally as large but slopes significantly less for the flat terrain spectra and for the vertical component. No obvious relationship existed between spectral shape and altitude or wind direction.

The frequency of turbulence varied from 2.7% to 4.6% for flights over flat terrain and high mountains, respectively. Above 60,000 ft. moderate turbulence was not uncommon over mountains but rarely was noted over low relief or water.

The fairly high number of turbulence cases above thunderstorm tops was largely influenced by location of base sites and by turbulence searching techniques. Consequently, thunderstorm turbulence was not classified separately.

These analyses resulted in suggested changes in the standard deviations of the root-mean-square gust velocities, the ratios of turbulent flight miles to total flight miles and the form of the power spectral density curves in current use for the design and operation of aircraft in the 45,000 to 65,000 ft altitude range.

TABLE OF CONTENTS

Section		Page
I	INTRODUCTION	1
II	PROBABILITY DENSITIES OF ROOT-MEAN-SQUARE GUST VELOCITIES	2
	Types of Root-Mean-Square Gust Velocities	2
	The HICAT Sample	2
	Selection of Sample	3
	Relationship Between Lateral, Longitudinal and Vertical RMS ( $\lambda = 2,000$ ft) Gust Velocities	4
	Probability Densities of the Root-Mean-Square Gust Velocities	6
	Effect of the Definition of Turbulence Upon the Standard Deviations of the Root-Mean-Square Gust Velocities	9
III	SCALE LENGTHS OF HIGH ALTITUDE CLEAR AIR TURBULENCE	22
	Mathematical Representation of Spectra	22
	Scale Lengths for the Total HICAT Sample	23
	Scale Lengths of Composite Spectra Representing Topographic and Altitude Categories	32
IV	STANDARD DEVIATION OF THE ROOT-MEAN-SQUARE GUST VELOCITY	35
	Introduction	35
	Estimating $b_1$ 's	36
V	RATIO OF TURBULENT FLIGHT MILES TO TOTAL FLIGHT MILES	40
	Definition of Turbulence	40
	Ratio of Turbulent Flight Miles to Total Flight Miles for Categories of Altitude, Topography and Season	41



TABLE OF CONTENTS (Continued)

Section		Page
VI	TURBULENCE ABOVE THUNDERSTORMS	45
	Clear Air Turbulence Above Thunderstorms in the HICAT Program	45
	World-Wide Distribution of Thunderstorms	46
VII	WORLD-WIDE DISTRIBUTION OF TOPOGRAPHIC CATEGORIES	48
VIII	FREQUENCY OF OCCURRENCE OF TURBULENCE AS A FUNCTION OF HEADWIND AND TAILWIND	57
IX	POWER SPECTRAL DENSITY CURVES AS FUNCTION OF AIRCRAFT HEADING WITH RESPECT TO WIND DIRECTION	59
	Introduction	59
	High Mountains	59
	Low Mountains	59
	Flatland	60
	Summary	60
X	DISTRIBUTION OF TRUE GUST VELOCITIES	62
	Introduction	62
	Distribution of the True Gust Velocities for HICAT Flight 280, Run 11	62
XI	SUMMARY AND CONCLUSIONS	64
	APPENDIX I	66
	REFERENCES	68

LIST OF ILLUSTRATIONS

Figure		Page
1	Comparison by Component and Altitude of Probability Density of RMS ( $\lambda = 2,000$ ft) - $\bar{x}$ .	11
2	Comparison by Altitude and Component of Probability Density of RMS ( $\lambda = 2,000$ ft) - $\bar{x}$ .	12
3	Comparison by Component and Underlying Topography of the Probability Densities of RMS ( $\lambda = 2,000$ ft) - $\bar{x}$ .	13
4	Comparison by Underlying Topography and Component of the Probability Densities of RMS ( $\lambda = 2,000$ ft) - $\bar{x}$ .	14
5	Comparison by Component of the Probability Densities of all Cases of RMS ( $\lambda = 2,000$ ft) - $\bar{x}$ .	15
6	Probability of RMS ( $\lambda = 2,000$ ft) - $\bar{x}$ Equalling or Exceeding Given Magnitudes	16
7	Probability of RMS ( $\lambda = 2,000$ ft) - $\bar{x}$ Equalling or Exceeding Given Magnitudes	17
8	Probability of RMS ( $\lambda = 2,000$ ft) - $\bar{x}$ Equalling or Exceeding Given Magnitudes	18
9	Probability of RMS ( $\lambda = 2,000$ ft) - $\bar{x}$ Equalling or Exceeding Given Magnitudes	19
10	Probability of RMS ( $\lambda = 2,000$ ft) - $\bar{x}$ Equalling or Exceeding Given Magnitudes	20
11	Probability of RMS ( $\lambda = 2,000$ ft) - $\bar{x}$ Equalling or Exceeding Given Magnitudes	21
12 a, b,c, d	Comparison of Taylor-Bullen, Sharp-Knee and Mild-Knee Equations for Different Values of L	24
12 e	Comparison of Taylor-Bullen, Sharp-Knee and Mild-Knee Equations for Different Values of L	25
13	Scale Length, L, as a Function of the Ratio of Root-Mean-Square Gust Velocities and Slope, m, for the Mild-Knee Equation. (Shaded Areas Indicate Effects of 2% and 5% Uncertainties in the Abscissa and Ordinate Values)	27

LIST OF ILLUSTRATIONS (Cont.)

Figure		Page
14	Scale Length, L, as a Function of the Ratio of Root-Mean-Square Gust Velocities and Slope, m, for the Mild-Knee Equation. (Shaded Areas Indicate Effects of 2% and 5% Uncertainties in the Abscissa and Ordinate Values)	28
15	Spectra, Slopes and Scale Lengths for the Total HICAT Sample	31
16	Comparison of Normalized Composite Spectra Separated by Intensity of the Turbulence	31
17a,b,c	Composite Spectra for Topographic Categories	33
18a,b,c	Composite Spectra for Altitude Categories	34
19	North America - Relief Differences	49
20	South America - Relief Differences	50
21	Europe - Relief Differences	51
22	Asia - Relief Differences	52
23	Australia - Relief Differences	53
24	Africa - Relief Differences	54
25	Southeast Asia - Relief Differences	55
26a	Japan - Relief Differences	56
26b	Hawaii - Relief Differences	56
27	(A) Frequency of Occurrence of 264 Runs by Wind Direction; (B) Percent of Time in Turbulence by Aircraft Heading; and (C) Percent of Time in Turbulence by Aircraft Heading - Wind Direction Difference	58
28a,b	Power Spectral Density Curves for Various Aircraft Headings-High Mountains	60
28c,d	Power Spectral Density Curves for Various Aircraft Headings-Low Mountains	61
28e,f	Power Spectral Density Curves for Various Aircraft Headings-Flatland	61
29	Distribution of True Gust Velocities for Three Components-Flight 280, Run 11	63

LIST OF TABLES

Table		Page
I	Number of RMS Gust Velocities Computed for Various Truncation Limits	2
II	Distribution of RMS ( $\lambda = 2,000$ ft) Cases by Season, Terrain and Altitude	3
III	Correlation Coefficients Between Components of Gust Velocity	5
IV	Slopes (m) and Intercepts (B) Obtained from Linear Regression Equations Relating RMS ( $\lambda = 2,000$ ft) Gust Velocity Components	7
V	Standard Deviations of RMS ( $\lambda = 2,000$ ft) Gust Velocities	8
VI	Comparison of Standard Deviations of RMS ( $\lambda = 2,000$ ft) When $\bar{x} = 0.50$ and $\bar{x} = 1.00$ ft/sec for the Various Components	10
VII	RMS ( $2.5 \times 10^{-4}$ cycles/ft.)/RMS ( $10^{-3}$ cycles/ft.) for the Mild-Knee Equation (Equation 7)	25
VIII	RMS ( $10^{-4}$ cycles/ft)/ RMS ( $10^{-3}$ cycles/ft) for the Mild-Knee Equation (Equation 7)	26
IX	Range in Computed Values of Scale Length for Various Errors in m and Ratio of the Root-Mean-Square Gust Velocities	29
X	Slopes and Scale Lengths of Composite Spectra (Minimum $\Omega = 10^{-4}$ cycles/ft) (Crooks, et al (2) ).	30
XI	Scale Lengths of Composite Spectra	32
XII	Ratio of $\sigma$ to Root-Mean-Square Gust Velocity from Spectra Truncated at $5 \times 10^{-4}$ Cycles/Ft (Based on Mild-Knee Equation)	37
XIII	Values of s, L, m, $b_1$ and $\bar{x}$ For High Altitude Clear Air Turbulence	38
XIV	Ratio of Turbulent Flight Miles to Total Flight Miles	42
XV	Comparison of Steiner (NASA U-2), HICAT and MIL-A-8861A Data	43
XVI	Recommended Ratios of Turbulent Flight Miles to Total Flight Miles	43

LIST OF TABLES (Cont.)

Table		Page
XVII	Number of Occurrences by Terrain of Turbulence with Vertical RMS Greater than Listed Values for Given Altitude Bands	44
XVIII	Flight Miles by Season for Four Terrain Types (HICAT Flights 54 to 285)	44
XIX	Percentage Flight Miles with Turbulence $\geq$ Light (cg peaks $> + 0.10g$ ) and Moderate in Parenthesis (cg peaks $> + 0.25g$ ) by Season for Four Terrain Types (HICAT Flights 54 to 285)	44
XX	Characteristics of Turbulence Above Thunderstorms	45

## SYMBOLS

a	Area of turbulent region (Eq. 9)
b	Constant (Eqs. 4 and 5)
$b_1$	Standard deviation of root-mean-square gust velocity in non-storm turbulence [ft/sec]
$b_2$	Standard deviation of root-mean-square gust velocity in storm turbulence [ft/sec]
F	Proportion of total area covered by turbulent regions associated with thunderstorms (Eqs. 9 and 10)
K	Number of turbulent regions (Eq. 9)
L	Scale length (Eqs. 4 through 7) [ft]; also length of turbulent region (Eq. 9)
m	Slope of power spectra <sup>1</sup> density high frequency asymptote on a log-log plot.
$m_1, m_2, m_3$	Slopes of linear regression equations relating RMS gust velocity components (Eq. 1)
n	Number of thunderstorm days per unit time; also constant (Eq. 4 and 5)
P	Probability
P( )	Probability density function [ (ft/sec) <sup>2</sup> /cycles/ft]
$P_1$	Proportion of flight miles in non-storm turbulence
$P_2$	Proportion of flight miles in storm turbulence
s	Standard deviation of root-mean-square gust velocity [ft/sec]
$t_1$	Ratio of time interval for n thunderstorms to thunderstorm duration
$U_{de}$	Derived equivalent gust velocity [ft/sec]
$U_F$	Longitudinal gust component measured in the horizontal plane parallel to the average heading of the aircraft over the duration of a run [ft/sec]

SYMBOLS (Continued)

$U_L$	Lateral gust component measured in the horizontal plane perpendicular to the average heading of the aircraft over the duration of a run [ft/sec]
$U_V$	Vertical gust component measured perpendicular to the horizontal plane [ft/sec]
$x$	Truncated root-mean-square gust velocity [ft/sec]
$\bar{x}$	Minimum or threshold root-mean-square gust velocity [ft/sec]
$\theta_1, \theta_2, \theta_3$	Intercepts of linear regression equations relating RMS gust velocity equations (Eq. 1) [ft/sec]
$\lambda$	Wavelength [ft]
$\sigma$	Root-mean-square gust velocity [ft/sec]
$\sigma_T$	$\sigma - \bar{x}$
$\phi( )$	Power spectrum density function
$\Omega$	Spatial frequency [cycles/ft]

## SECTION I

### INTRODUCTION

This report consists of a discussion of those characteristics of high altitude clear air turbulence that are of direct interest to those engaged in the design and operation of advanced aircraft. Specifically, the probability density distribution of the root-mean-square gust velocities, the proportion of flight miles in turbulence, and the scale of turbulence are given as functions of altitude and underlying topography. Factors such as the "scale length of the turbulence", distribution of gust velocities, turbulence above thunderstorm clouds and the relation between clear air turbulence and the flight direction with respect to the wind and mountain ridges are discussed in detail.

The results presented in this report were obtained through the use of statistical and theoretical analyses of the complete set of data from the HICAT flight program. In many instances the data published by Crooks, et al. (1,2) were supplemented with unpublished data.

The general organization of this report is as follows. First, the probability density distributions of the root-mean-square gust velocities obtained from truncated power spectral density curves were determined for the entire HICAT sample and for the sample divided into altitude and topographic categories. Next, the shape, slope, and associated turbulence "scale lengths" of the power spectral density curves were determined.

Once the appropriate mathematical representations of the spectra were obtained, the relationship was established between the total root-mean-square gust velocities and the root-mean-square gust velocities obtained from the truncated spectra. This led directly to the probability density distributions of the total root-mean-square gust velocities. The standard deviations of these velocities gives the "b's" for the equations commonly used by structural engineers. Then the proportion of flight time in turbulence (the "P's" of the equations used by the engineers) are given. The remainder of the report discusses other characteristics of high altitude turbulence.



## SECTION II

### PROBABILITY DENSITIES OF ROOT-MEAN-SQUARE GUST VELOCITIES

#### Types of Root-Mean-Square Gust Velocities

Two different values of the root-mean-square gust velocities have been found to be useful for the design and operation of aircraft. One of these values corresponds to the square root of the area under the power spectral density curve between wavelength (frequency) limits that are within the range of the measurements. The second value of the root-mean-square gust velocity frequently used is given by the square root of the area under the complete spectrum. This is the value used in most analytical representations of the gust velocities. Procedures for estimating the total areas if the areas under the truncated curves are known are discussed in Section IV.

#### The HICAT Sample

In the HICAT program the turbulent regions varied in length from approximately 1 to 115 nautical miles. The distribution of the lengths of the turbulent regions is discussed in detail by Ashburn et al. (3) and Ashburn (4). The procedure that was adopted for computing the spectra required that the largest wavelength in the spectra be represented by at least twenty samples. Thus, the long wave limits of the computed spectra were determined by the observed lengths of the turbulent regions. The lower wavelength limit of approximately 130 ft. was determined largely by the response of the instruments, the speed of the aircraft and needs of the designers of aircraft. The root-mean-square gust velocities were computed from the spectra with the long wavelength limits set at 1,000 ft., 2,000 ft., 4,000 ft., 10,000 ft., and 20,000 ft. for all turbulent regions whose length was at least 20 times the long wavelength limit.

The size of the sample of root-mean-square gust velocities decreased significantly as the upper truncation line was moved to longer wavelengths. This is shown in Table I.

TABLE I

Number of RMS Gust Velocities Computed for Various Truncation Limits

Upper Wavelength Truncation Limit	Number of Cases
2,000 ft. [ RMS ( $\lambda = 2,000$ ft) ]	197
4,000 ft. [ RMS ( $\lambda = 4,000$ ft) ]	116
10,000 ft. [ RMS ( $\lambda = 10,000$ ft) ]	46
20,000 ft. [ RMS ( $\lambda = 20,000$ ft) ]	9

The criteria for each of the cases listed in Table I were:

- a) The RMS ( $\lambda = 2,000$  ft) gust velocity for the vertical component was equal to or greater than 0.5 ft/sec.
- b) Reliable spectra for all three gust velocity components were available.

The division by season, type of underlying terrain and altitude of the 197 cases of RMS ( $\lambda = 2,000$  ft) is given in Table II.

TABLE II

Distribution of RMS ( $\lambda = 2,000$  ft) Cases by Season, Terrain and Altitude

	Winter	Spring	Summer	Autumn	All Seasons
Water	2	11	18	0	31
Flatland	19	25	5	4	53
Low Mountains	17	4	0	13	34
High Mountains	37	14	0	28	79
All Terrain	75	54	23	45	197
45,000 to 49,900 ft	6	5	4	6	21
50,000 to 54,900 ft	34	15	15	6	70
55,000 to 59,900 ft	16	26	3	17	62
$\geq 60,000$ ft	17	8	0	16	41

Selection of Sample

The distribution of lengths of the turbulent regions encountered in the HICAT flight program (Ashburn, 4) was such that approximately 85% of the turbulent regions were long enough to permit the computation of RMS ( $\lambda = 2,000$  ft) under

the criteria established by Crooks et al., (1, 2). The corresponding percentages for RMS ( $\lambda = 10,000$  ft) and RMS ( $\lambda = 20,000$  ft), where there had been no malfunctions of instruments, were approximately 20% and 5%, respectively. These data, along with the results presented in Tables I and II, indicate that if a statistical summary of the RMS gust velocities is to be made by categories of underlying terrain, season or altitude, then only the RMS ( $\lambda = 2,000$  ft) values provide an adequate sample size. Selecting the RMS ( $\lambda = 2,000$  ft) values for the analysis has some obvious disadvantages from the point of view of studying important characteristics of the spectra but this choice had to be made if the root-mean-square gust velocities were to be investigated as functions of altitude, season and terrain.

Relationship Between Lateral, Longitudinal and Vertical RMS ( $\lambda = 2,000$  ft) Gust Velocities

Correlation coefficients,  $r$ , between the lateral-vertical, longitudinal-vertical, and the lateral-longitudinal RMS ( $\lambda = 2,000$  ft) values were computed using the following relationship:

$$r = \frac{n \sum x_i y_i - \sum x_i \sum y_i}{\sqrt{[n \sum x_i^2 - (\sum x_i)^2] [n \sum y_i^2 - (\sum y_i)^2]}}$$

where the summations are taken from  $i = 1$  to  $i = n$  and the  $x_i$  and  $y_i$  are the appropriate RMS ( $\lambda = 2,000$  ft) values. The results given in the second column of Table III were obtained by giving equal weight to the values published by Crooks et al (1, 2). The results given in the first column were obtained by weighting each value according to the length of the time in turbulence. For example, a turbulent region that lasted for 500 seconds of flight time was given five times the weight of a turbulent region that was traversed in 100 seconds. If the turbulence that lasted 500 seconds was stationary in character, then it could have been divided into five 100 second turbulent regions. This is the justification for weighting the RMS ( $\lambda = 2,000$  ft) values by the time in turbulence. In general there was no statistically significant difference between the results obtained by no weighting and weighting. The relatively high correlation coefficients given in Table III suggest that the components of RMS ( $\lambda = 2,000$  ft) are linearly related and hence may be represented by

$$\begin{aligned} \text{RMS } (\lambda = 2,000 \text{ ft})_L &= m_1 \text{ RMS } (\lambda = 2,000 \text{ ft})_V + \beta_1 \\ \text{RMS } (\lambda = 2,000 \text{ ft})_F &= m_2 \text{ RMS } (\lambda = 2,000 \text{ ft})_V + \beta_2 \\ \text{RMS } (\lambda = 2,000 \text{ ft})_L &= m_3 \text{ RMS } (\lambda = 2,000 \text{ ft})_F + \beta_3 \end{aligned} \quad (1)$$

TABLE III

Correlation Coefficients Between Components of Gust Velocity

			Correlation Coefficients	
			Weighted by Time In Turbulence	Non-Weighted
Underlying Topography	Water	Lateral-Vertical	.899	.938
		Longitudinal-Vertical	.796	.835
		Lateral-Longitudinal	.793	.847
	Flatland	Lateral-Vertical	.965	.937
Longitudinal-Vertical		.942	.908	
Lateral-Longitudinal		.946	.919	
Low Mountains	Lateral-Vertical	.870	.845	
	Longitudinal-Vertical	.883	.890	
	Lateral-Longitudinal	.896	.870	
High Mountains	Lateral-Vertical	.966	.960	
	Longitudinal-Vertical	.962	.962	
	Lateral-Longitudinal	.964	.960	
All Cases		Lateral-Vertical	.955	.950
		Longitudinal-Vertical	.953	.950
		Lateral-Longitudinal	.950	.944
Flight Altitude	45,000 to 49,900 Ft	Lateral-Vertical	.938	.950
		Longitudinal-Vertical	.948	.961
		Lateral-Longitudinal	.867	.881
	50,000 to 54,900 Ft	Lateral-Vertical	.963	.963
Longitudinal-Vertical		.964	.963	
Lateral-Longitudinal		.947	.947	
55,000 to 59,900 Ft	Lateral-Vertical	.967	.943	
	Longitudinal-Vertical	.958	.946	
	Lateral-Longitudinal	.958	.940	
60,000 Ft and Above	Lateral-Vertical	.951	.951	
	Longitudinal-Vertical	.955	.954	
	Lateral-Longitudinal	.971	.971	

The values of  $m_1$ ,  $m_2$ ,  $m_3$ ,  $\beta_1$ ,  $\beta_2$  and  $\beta_3$  are given in Table IV. These values may be used for two purposes. First, they relate to the problem of estimating the degree of isotropy of the turbulence. Secondly, if the existence of turbulence is defined in terms of the vertical component of the RMS ( $\lambda = 2,000$  ft) then equations (1) may be used to establish the definition of turbulence in terms of the lateral and longitudinal components.

The data presented in Table IV supplement the detailed discussion of the ratios of the components of the root-mean-square gust velocities that was given by Crooks et al. (1) by presenting an analysis of a larger sample and by dividing the sample into altitude and terrain categories. This new analysis indicates that the ratio of any two of the components of RMS ( $\lambda = 2,000$  ft) is not a constant but varies with the magnitude of the root-mean-square gust velocities. Further, the analysis indicates that the relationship between any two of the components changes significantly with altitude and terrain category.

The values given in Table IV may be looked upon as useful in providing the best estimate of the relative magnitudes of the components of RMS ( $\lambda = 2,000$  ft). The relationships between the components of  $\sigma$  are given in Section III.

#### Probability Densities of the Root-Mean-Square Gust Velocities

The probability densities of the root-mean-square gust velocities obtained from the HICAT program may be represented by histograms or by analytical functions. The histograms represent the data more directly. Analytical functions are more convenient to use but present difficulties, 1) in the attempt to determine if the analytical functions satisfactorily fit the data and 2) in determining the value of using the analytical function beyond the range of the data.

In the effort to determine the probability densities of the HICAT root-mean-square gust velocities the following assumptions were made:

- a) The sample size was adequate for only the root-mean-square gust velocities computed from the spectra with the truncation limits 130 ft. and 2,000 ft.
- b) The analytic function is given by

$$P(x) = \frac{1}{s} \sqrt{\frac{2}{\pi}} \exp\left(-\frac{(x-\bar{x})^2}{2s^2}\right) \quad (2)$$

where  $x$  represents the root-mean-square gust velocity and hence can only be positive,  $\bar{x}$  is the minimum value of the root-mean-square gust velocity for the air to be considered turbulent, and  $s$  is the standard deviation of the root-mean-square gust velocity.

- c)  $\bar{x} = 0.5$  ft/sec for the vertical component and  $\bar{x} = 0.5m_1 + \beta_1$  ft/sec

TABLE IV

Slopes (m) and Intercepts (s) Obtained from Linear Regression Equations  
Relating RMS ( $\lambda = 2,000$  ft) Gust Velocity Components\*

	$m_1(U_L U_V)$	$s_1(U_L U_V)$	$m_2(U_F U_V)$	$s_2(U_F U_V)$	$m_3(U_L U_F)$	$s_3(U_L U_F)$
Water	1.15 (1.19)	0.29 (0.25)	0.93 (0.88)	0.39 (0.45)	1.18 (1.29)	-0.13 (-0.27)
Flatland	1.18 (1.09)	0.27 (0.34)	0.90 (0.84)	0.33 (0.39)	0.95 (1.16)	-0.06 (-0.01)
Low Mountains	1.10 (0.96)	0.19 (0.35)	1.04 (0.93)	0.23 (0.36)	1.04 (0.98)	-0.03 (0.06)
High Mountains	0.99 (1.01)	0.30 (0.30)	1.00 (0.96)	0.30 (0.30)	0.96 (1.02)	0.16 (0.06)
Total Cases	1.00	0.36	0.96	0.27	0.98	0.15
45,000 - 49,900 ft	1.07	0.35	0.86	0.40	1.09	0.04
50,000 - 54,900 ft	1.04	0.41	0.96	0.31	1.04	0.12
55,000 - 59,900 ft	0.92	0.35	0.92	0.25	0.91	0.21
$\geq 60,000$ ft	1.07	0.21	1.06	0.18	0.98	0.06

\*Numbers in parentheses are for all observations given equal weight. All other numbers are based upon weighting observations according to length of time in turbulence.

for the lateral component and  $\bar{x} = 0.5m_2 + \beta_2$  ft/sec for the longitudinal component. The values of  $m_1$ ,  $m_2$ ,  $\beta_1$  and  $\beta_2$  are taken from Table IV.

- d) The standard deviations of the root-mean-square gust velocities derived from the HICAT data are as given in Table V.

\*TABLE V

Standard Deviations of RMS ( $\lambda = 2,000$  ft)  
Gust Velocities

	Vertical Component	Lateral Component	Longitudinal Component	Number Seconds
Water	(0.597) 0.456	(0.801) 0.604	(0.505) 0.409	6210
Flatland	(0.564) 0.608	(0.634) 0.792	(0.480) 0.535	16845
Low Mountains	(0.879) 0.858	(0.859) 1.00	(0.817) 0.915	8137
High Mountains	(1.47) 1.25	(1.52) 1.27	(1.42) 1.27	19388
All Cases	.938	0.960	0.910	
45,000-49,900 ft.	0.610	0.690	0.484	5510
50,000-54,900 ft.	0.963	1.027	0.930	20095
55,000-59,900 ft.	0.897	0.830	0.832	15445
$\geq 60,000$ ft.	1.09	1.20	1.19	9900

\* Figures in parentheses are based upon using equal weights for all turbulence observations. The other figures are based upon calculations weighting each observation by the time in turbulence.

The standard deviations based upon the weighting by the time in turbulence are the recommended ones because weighting each run equally distorts the contributions of the short runs.

The underlying topography appears to have a significant effect upon the standard deviation of the root-mean-square gust velocity. The figures presented in Table V indicate an increase in the standard deviation with an increase in surface roughness. The standard deviation for the lateral component is the largest for all of the categories of underlying topography. For the water and flatland categories the longitudinal component has the smallest standard deviation but as the terrain becomes rougher the longi-

tudinal component increases relative to the vertical component.

The standard deviations for all three components are smallest in the 45,000 ft. to 50,000 ft. altitude band and greatest for the altitudes above 60,000 ft. This increase in the standard deviation with altitude does not hold in the 50,000 - 60,000 ft. altitude range. Almost all turbulence above 60,000 ft. altitude occurred over mountains and was generally more intense than the average turbulence encounter below 60,000 ft. The data are inadequate to make it possible to definitely separate the altitude effect from the terrain effect.

The probability densities of the root-mean-square gust velocities were computed from Equation 2 and the results are shown in Figures 1 - 5. It is important to note that these probability densities relate to the truncated spectra and not to the total spectra. The probability densities for the root-mean-square gust velocities derived from the total spectra are discussed in Section IV.

Figures 6 through 11 consist of exceedance curves of RMS ( $\lambda = 2,000$ ft) for each of the three components and for the four categories of underlying terrain. The straight lines are exceedance curves based upon the standard deviation computed from the HICAT data and the assumption that the distributions are normal. The standard deviations were computed by using both plus and minus values of RMS ( $\lambda = 2,000$  ft) -  $\bar{x}$ . These are the values given in Table V. The data points fit the normal distribution reasonably well except for the cases over water and the highest values of RMS ( $\lambda = 2,000$  ft) for the mountain cases. There are insufficient data at this time to make possible a definitive conclusion relating to these departures from normal. The sample size is relatively small. In this report the assumption will be made that the distribution of RMS ( $\lambda = 2,000$  ft) is normal.

If the distributions of RMS gust velocities are assumed to be normal for the classifications of terrain or altitude then the distribution for all cases put in one group cannot be normally distributed because the sum of two normal distributions with different standard deviations is not a normal distribution. The probability density distribution for all cases then would be represented by

$$P(d) = P_1 \sqrt{\frac{2}{\pi}} \frac{1}{s_1} e^{-\frac{U^2}{2s_1^2}} + P_2 \sqrt{\frac{2}{\pi}} \frac{1}{s_2} e^{-\frac{U^2}{2s_2^2}} + \dots \quad (3)$$

where the  $P_1, P_2, \dots, P_4$  would be the proportion of time in turbulence for either the terrain or altitude classifications and the  $s_1, s_2, \dots, s_4$  are the appropriate standard deviations.

Effect of the Definition of Turbulence Upon the Standard Deviations of the Root-Mean-Square Gust Velocities.

The results given in Table V were based upon  $\bar{x} = 0.5$  ft/sec for the vertical



component of RMS ( $\lambda = 2,000$  ft). If the definition of the lower bound of turbulence for this component is changed to  $\bar{x} = 1.0$  ft/sec then the standard deviations of the weighted values are as given in Table VI.

TABLE VI

Comparison of Standard Deviations of RMS ( $\lambda = 2,000$  ft)  
When  $\bar{x} = 0.50$  and  $\bar{x} = 1.00$  ft/sec for the Various Components

Underlying Terrain	Vertical Component		Lateral Component		Longitudinal Component	
	$\bar{x}$		$\bar{x}$		$\bar{x}$	
	0.50 ft/sec	1.00 ft/sec	0.50 ft/sec	1.00 ft/sec	0.50 ft/sec	1.00 ft/sec
Water	0.456	0.409	0.604	0.457	0.409	0.433
Flatland	0.608	0.445	0.792	0.543	0.535	0.451
Low Mountains	0.858	0.482	1.00	0.621	0.915	0.534
High Mountains	1.25	0.946	1.27	0.929	1.27	0.969

These data suggest that the standard deviation shows less variation with different  $\bar{x}$  values than with classifications. In this report  $\bar{x} = 0.5$  ft was used because an examination of the data indicated that this value appears to be in closer agreement with the definition of turbulence used by Steiner (5).

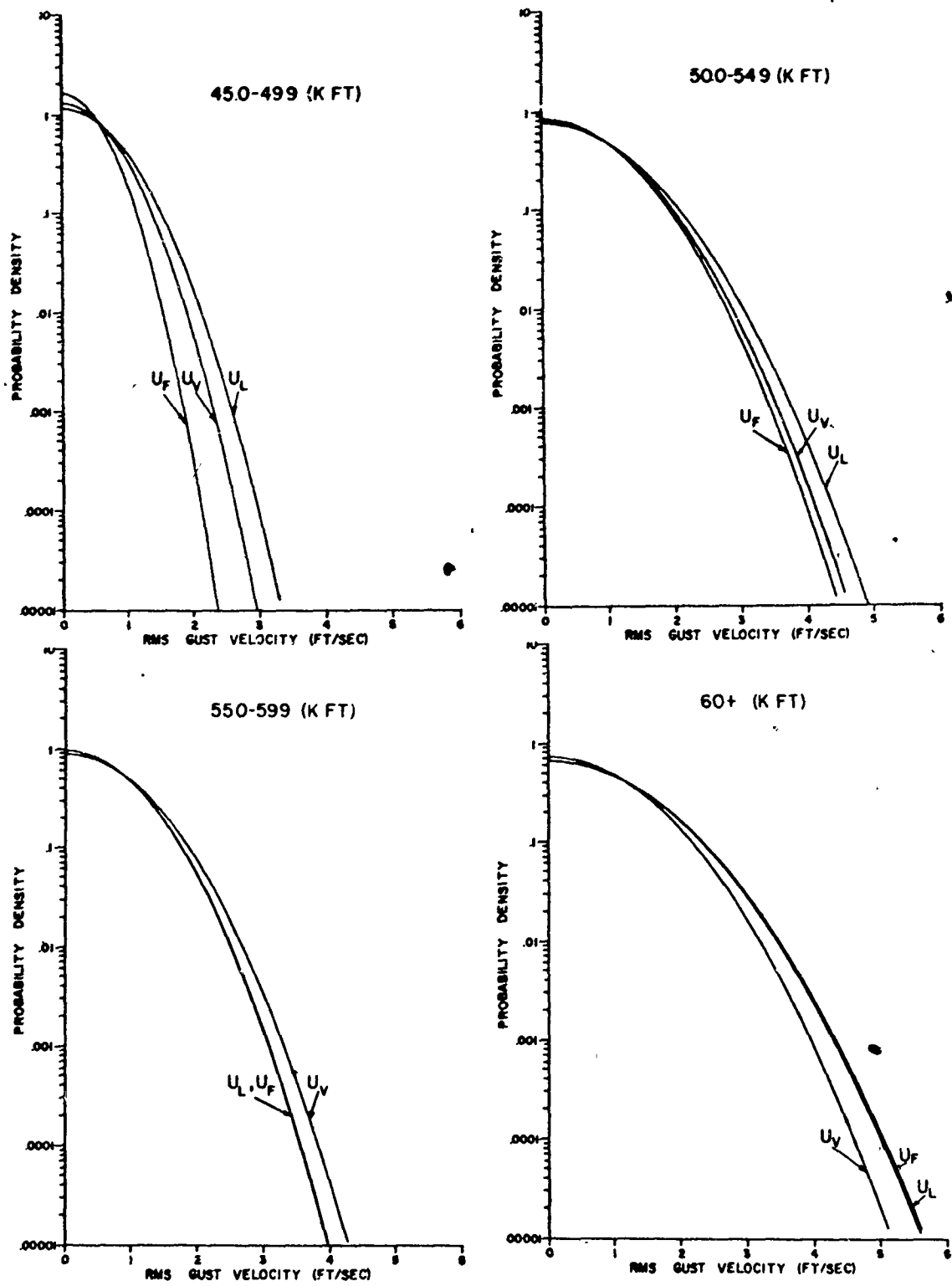


Figure 1. Comparison by Component and Altitude of Probability Density of RMS ( $\lambda = 2,000$  ft) -  $\bar{x}$ .

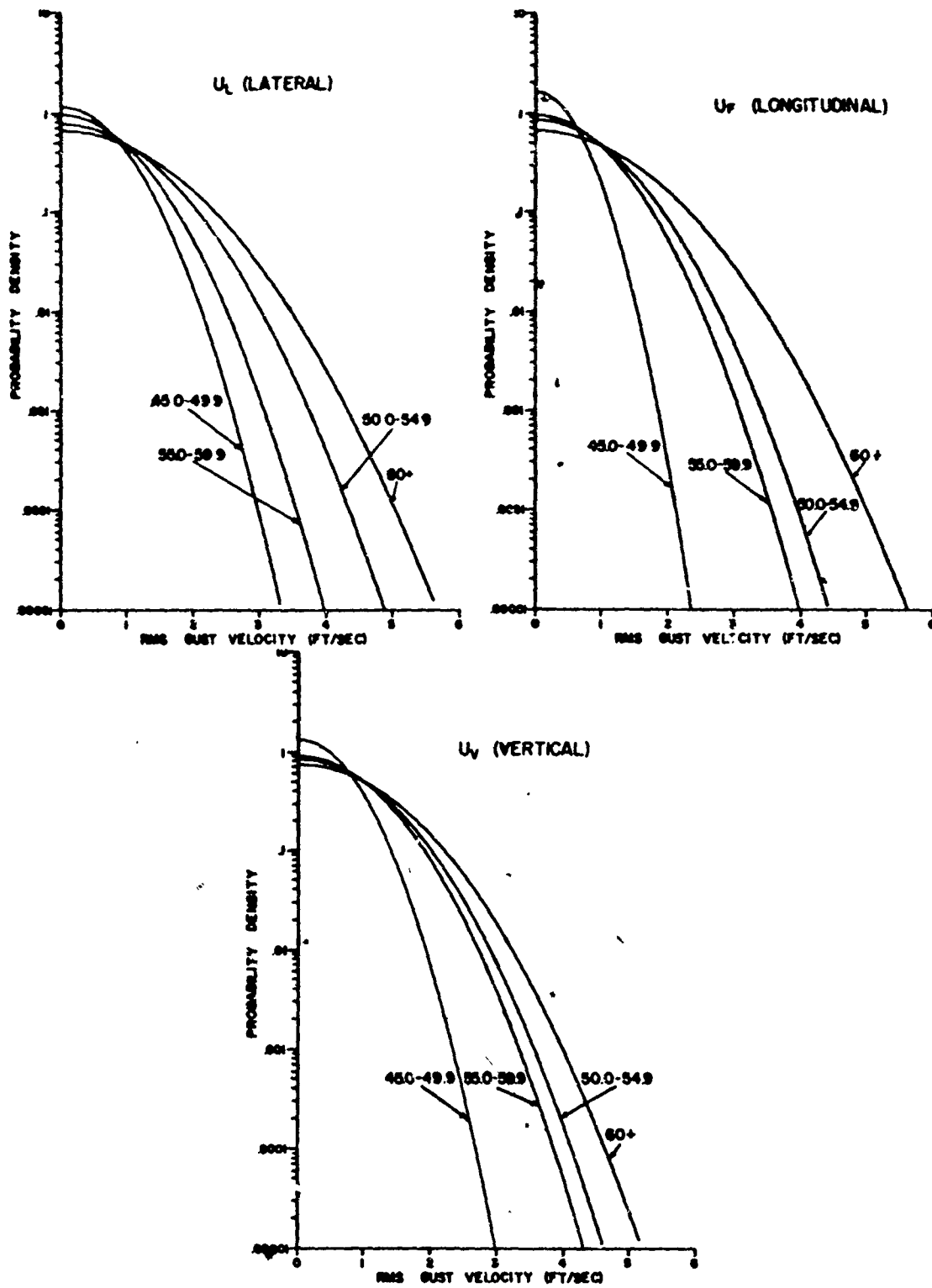


Figure 2. Comparison by Altitude and Component of Probability Density of RMS ( $\lambda = 2,000$  ft) -  $\bar{x}$ .

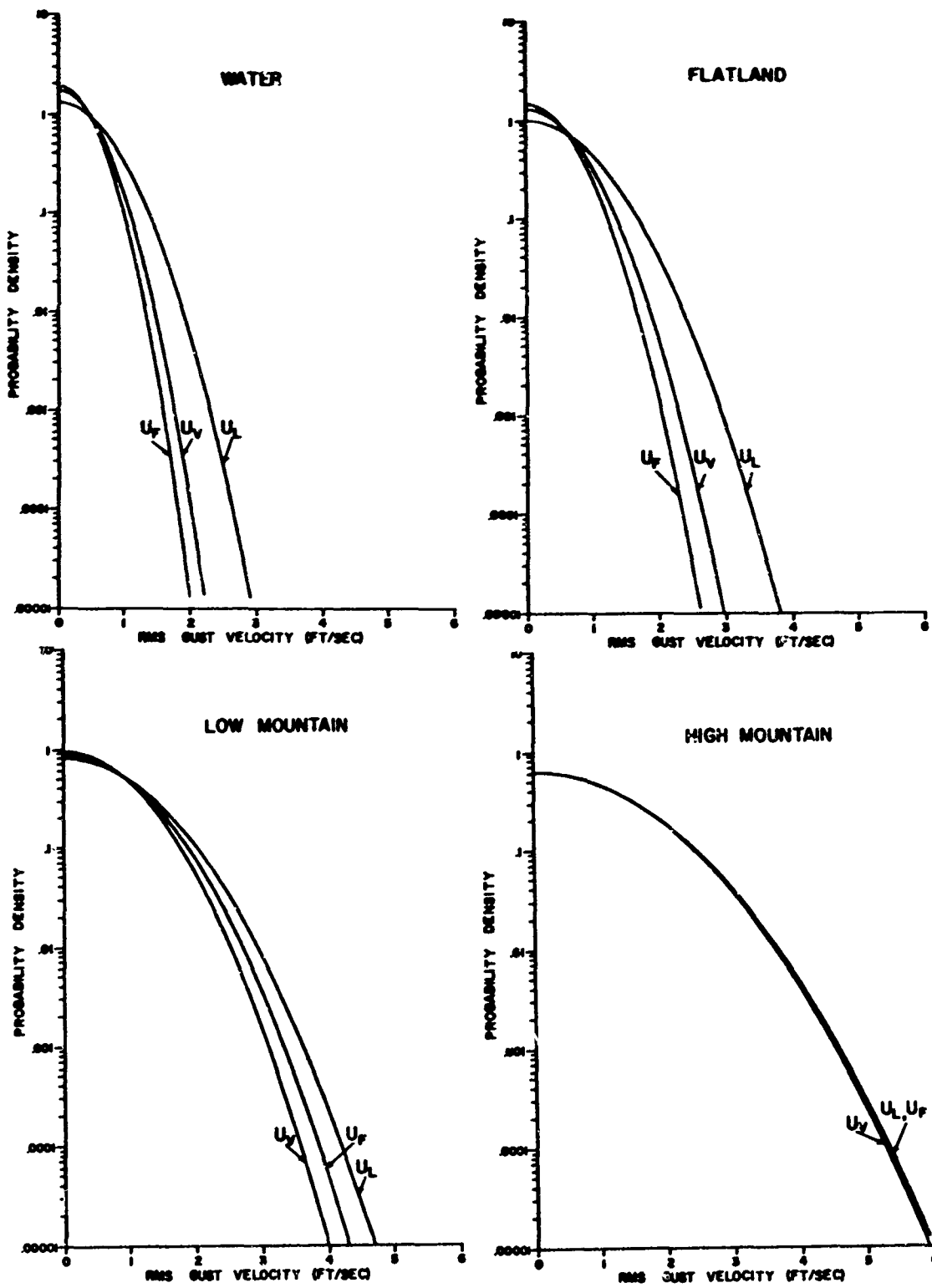


Figure 3. Comparison by Component and Underlying Topography of the Probability Densities of RMS ( $\lambda = 2,000$  ft) - x.

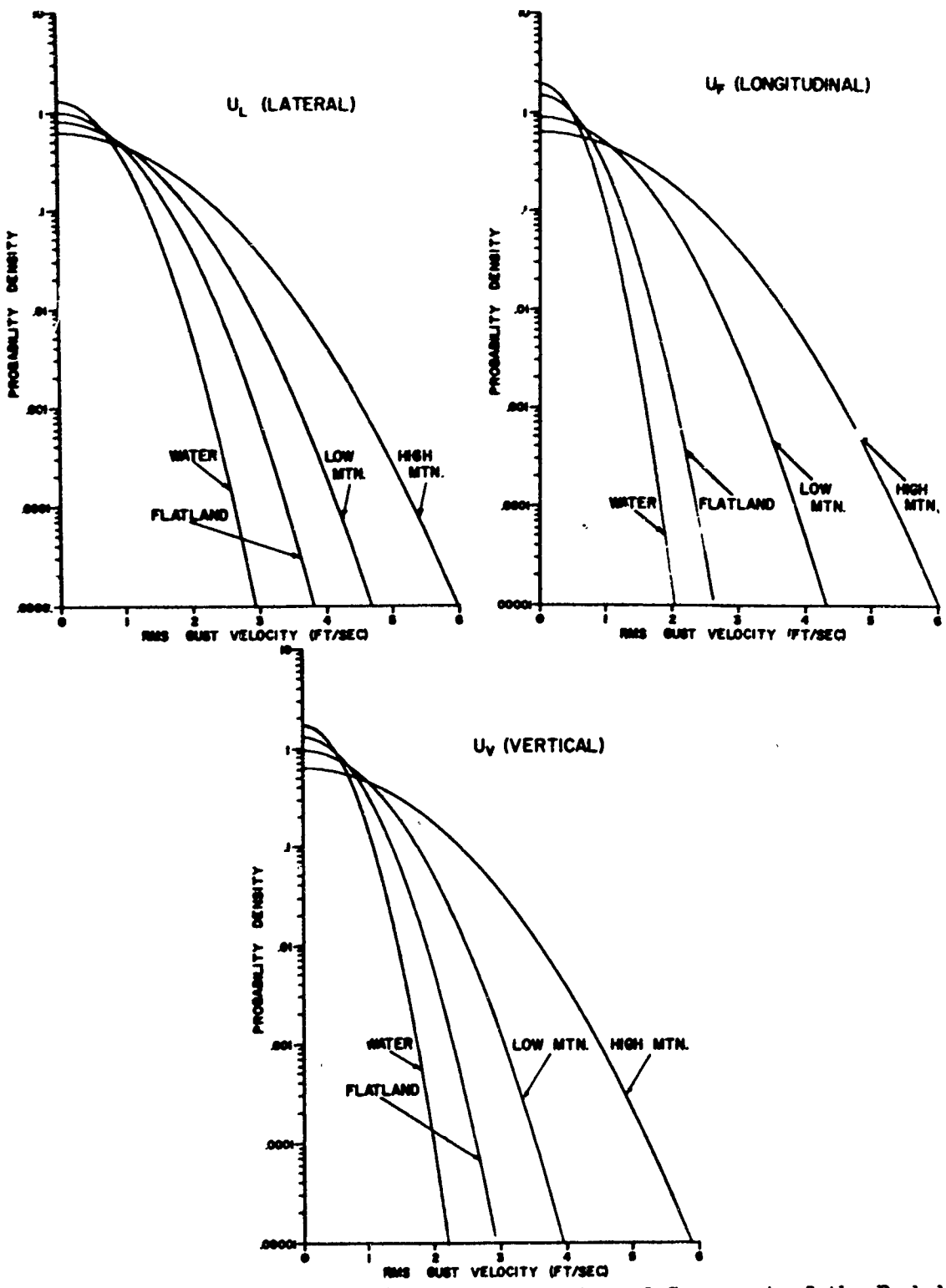


Figure 4. Comparison by Underlying Topography and Component of the Probability Densities of RMS ( $\lambda = 2,000$  ft) - X.

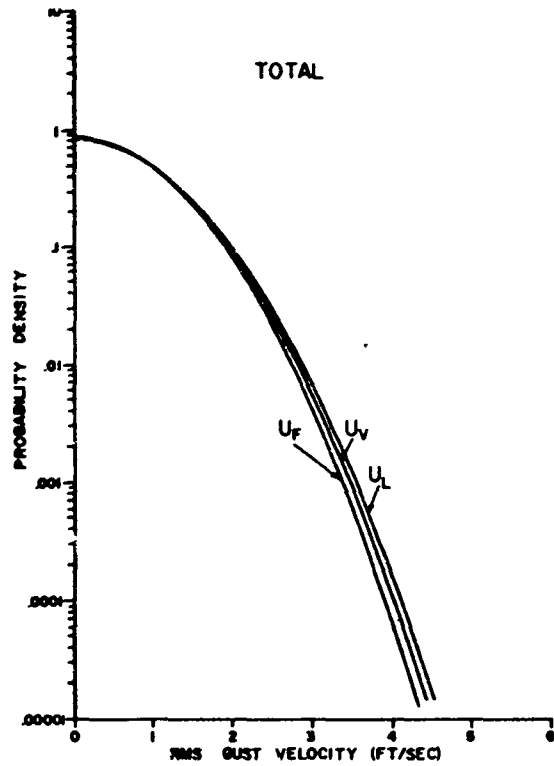


Figure 5. Comparison by Component of the Probability Densities of All Cases of RMS ( $\lambda = 2,000$  ft) -  $\bar{x}$ .

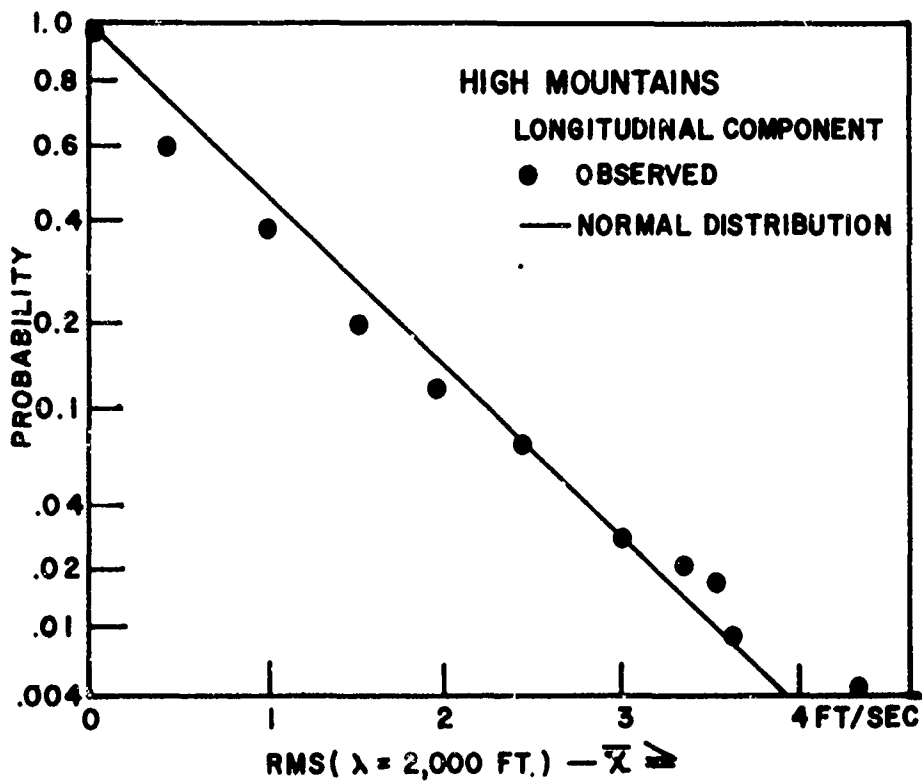
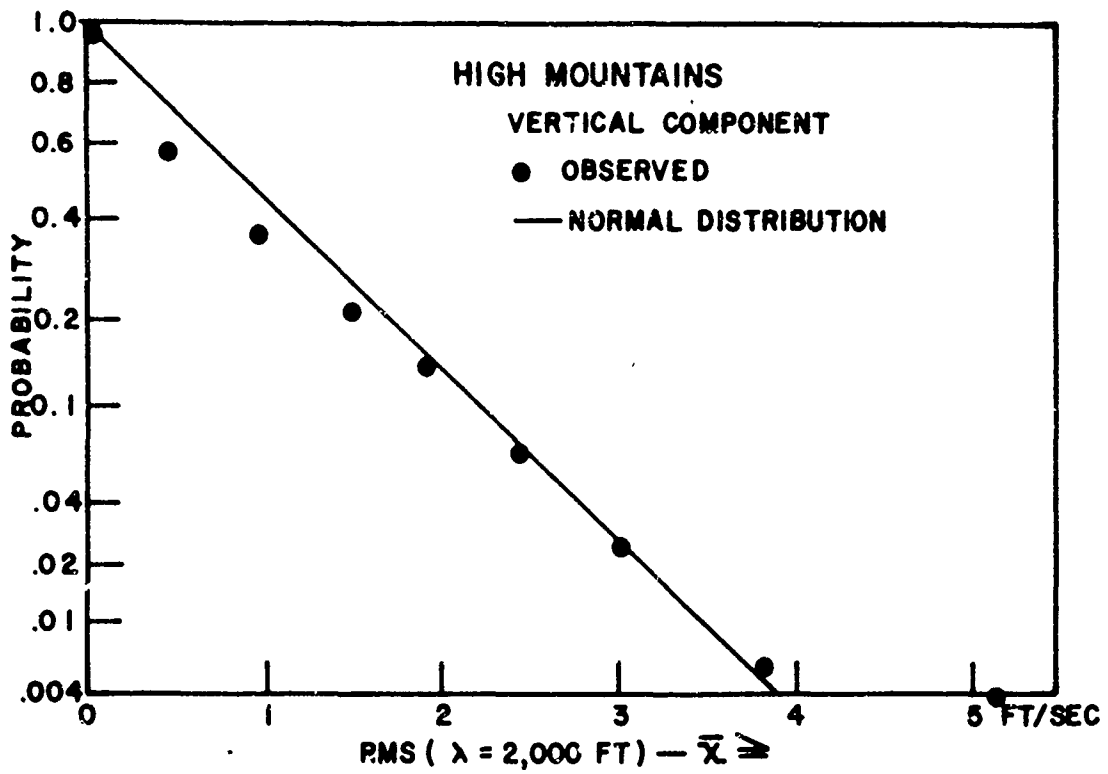


Figure 6. Probability of RMS ( $\lambda = 2,000$  ft) -  $\bar{x}$  Equalling or Exceeding Given Magnitudes

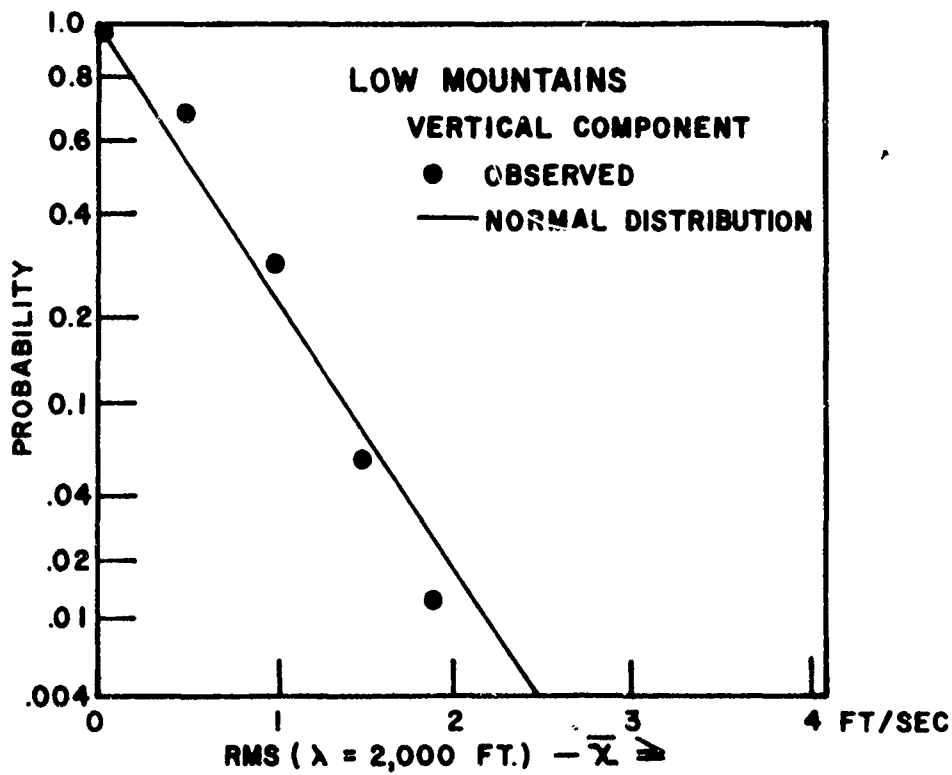
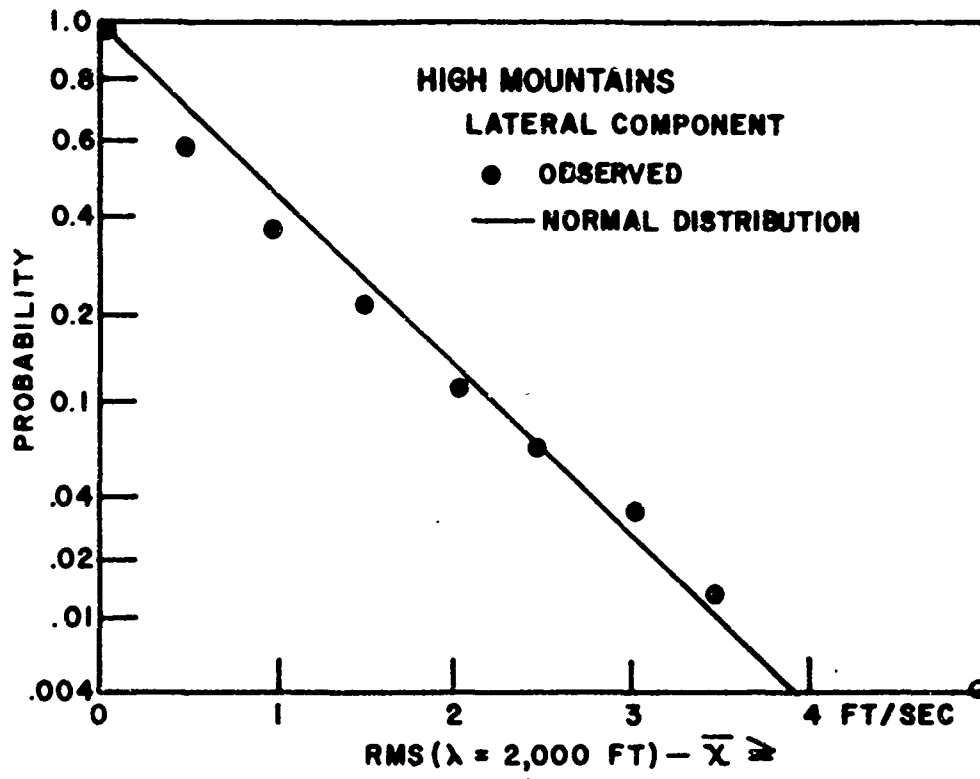


Figure 7. Probability of RMS ( $\lambda = 2,000$  ft) -  $\bar{x}$  Equalling or Exceeding Given Magnitudes



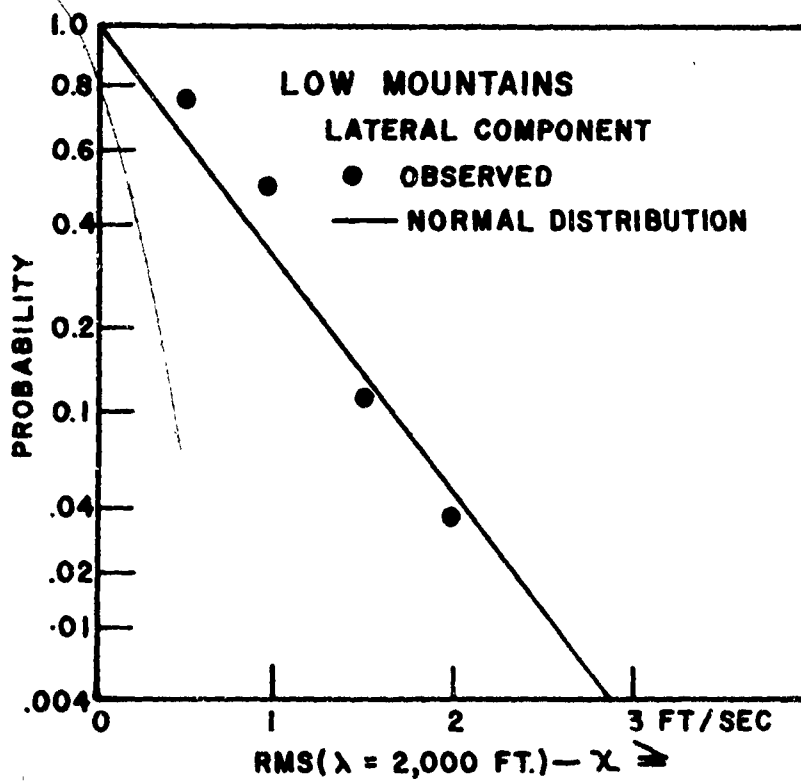
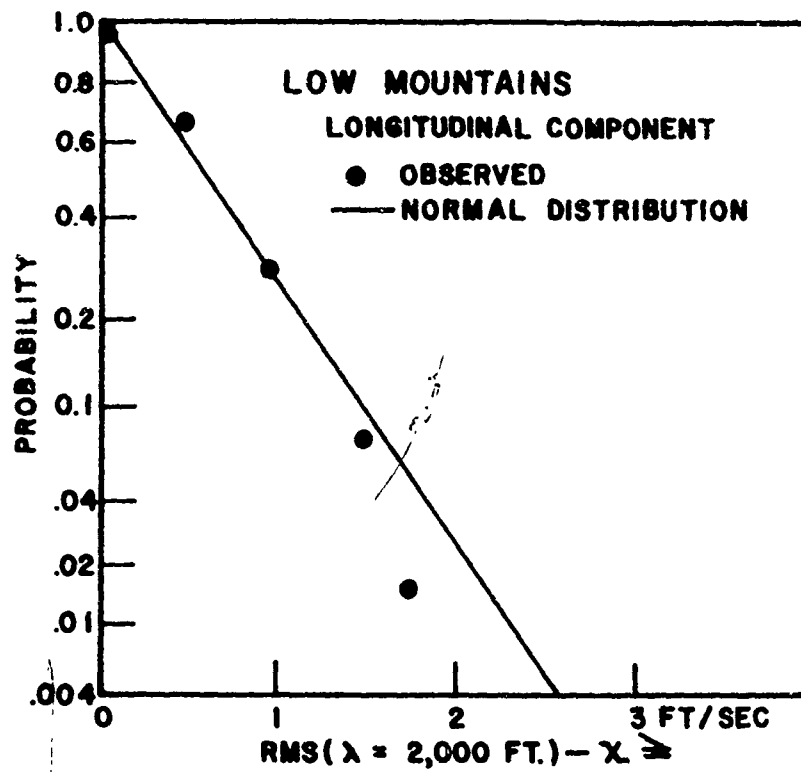


Figure 8. Probability of RMS ( $\lambda = 2,000$  ft) -  $\bar{x}$  Equalling or Exceeding Given Magnitudes

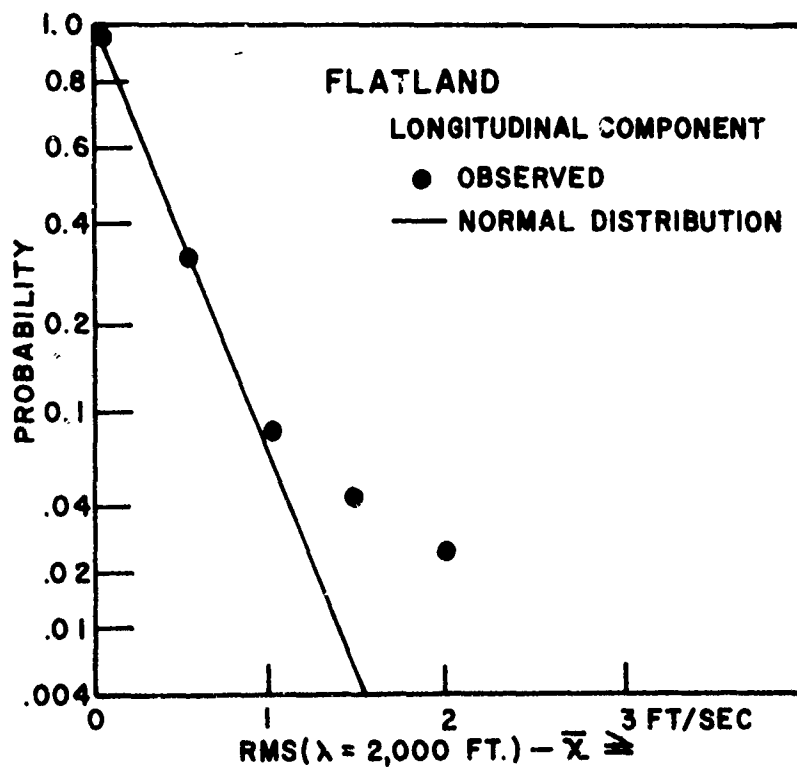
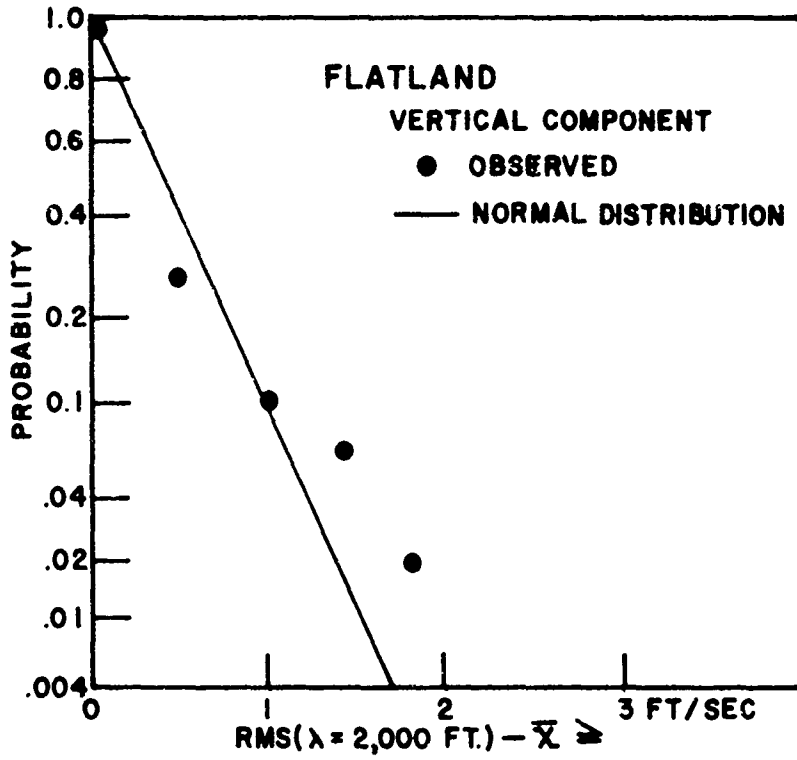


Figure 9. Probability of RMS ( $\lambda = 2,000$  ft) -  $\bar{x}$  Equalling or Exceeding Given Magnitudes

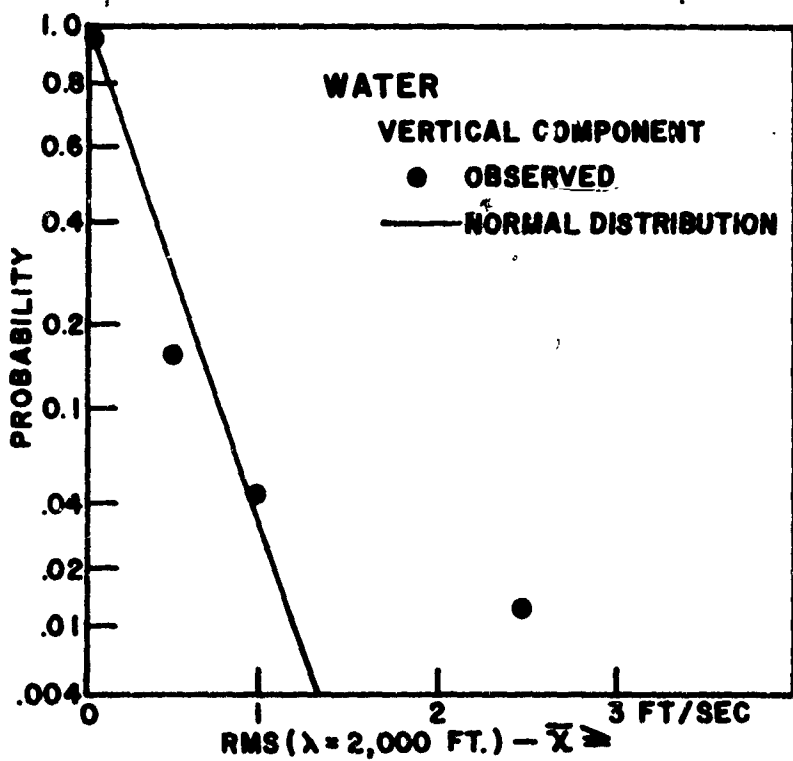
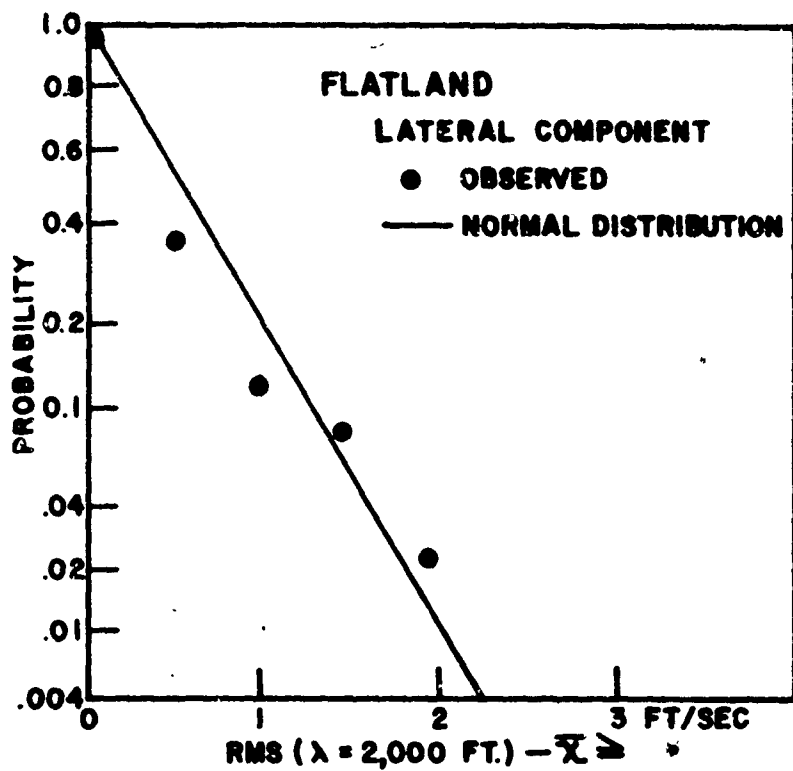


Figure 10. Probability of RMS ( $\lambda = 2,000$  ft) -  $\bar{x}$  Equalling or Exceeding Given Magnitudes

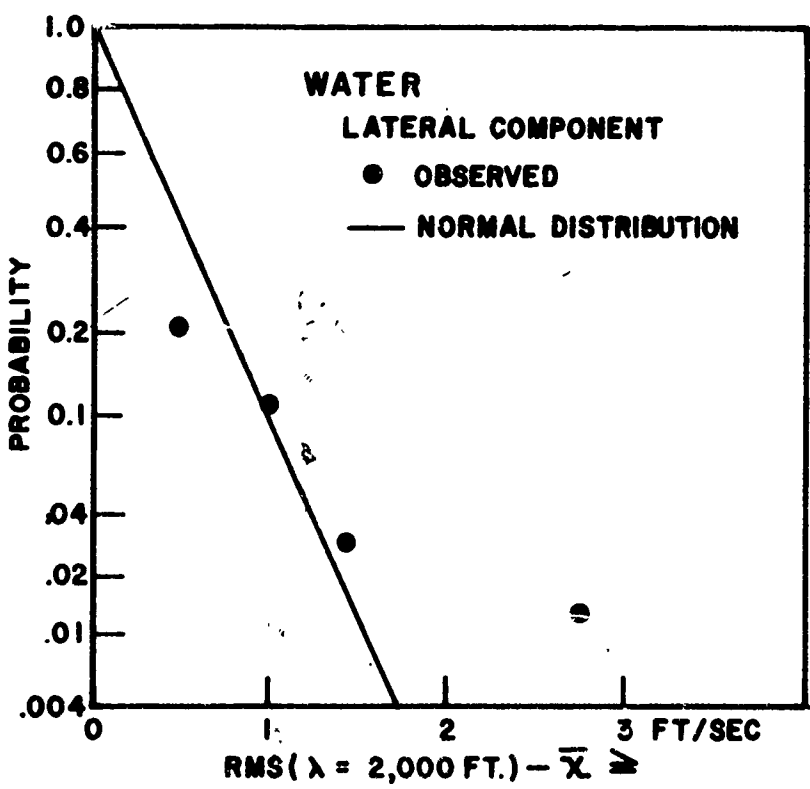
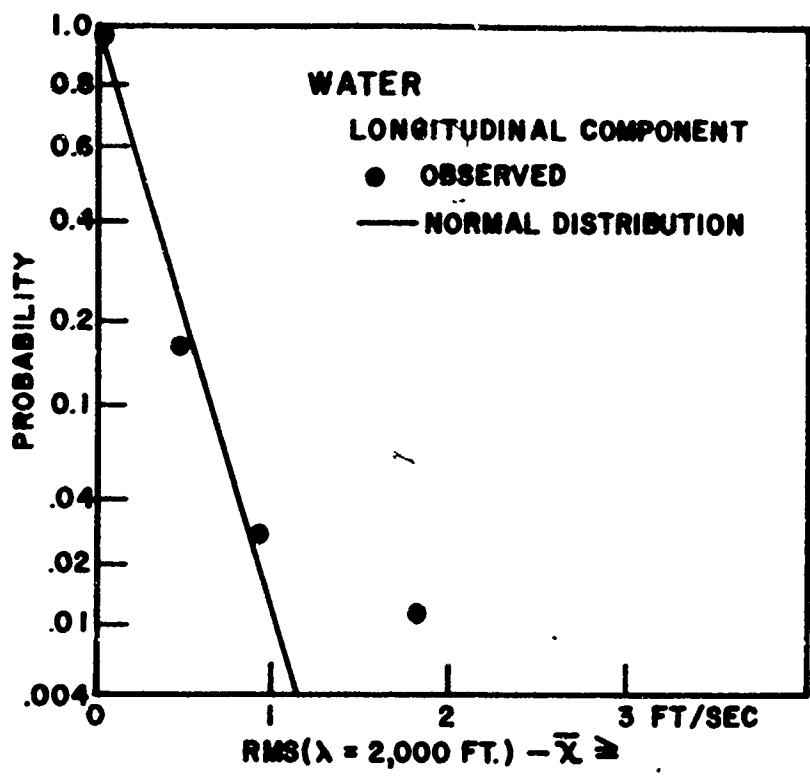


Figure 11. Probability of RMS ( $\lambda = 2,000$  ft) -  $\bar{x}$  Equalling or Exceeding Given Magnitudes

### SECTION III

#### SCALE LENGTHS OF HIGH ALTITUDE CLEAR AIR TURBULENCE

##### Mathematical Representation of Spectra

Current procedures for computing power spectral densities of measured gust velocities yield numerical values that define irregularly shaped power spectral density curves. Smooth curves obtained by "fairing" or by "least squares fit" are used to represent the principal features of these power spectral density curves. The mathematical expressions that are most frequently proposed to represent these smoothed power spectral density curves contain three parameters. One of these parameters, the root-mean-square gust velocity,  $\sigma$ , is a measure of the intensity of the turbulence and has the effect of moving the curve upward or downward in a direction parallel to the ordinate. The second parameter,  $m$ , determines the slope of the curve at the high frequency end. The third parameter, designated as the scale length,  $L$ , is a shape parameter that defines the rate of change of slope at the low frequency portion of the curve.

Crooks, Hoblit, and Mitchell (2) discuss in detail four families of functions that have been proposed to represent power spectral density curves. The first family includes both the Von Karman spectrum ( $m = -5/3$ )—and the Dryden spectrum ( $m = -2$ ) as special cases. The general form of the equation for this family, designated the Taylor-Bullen family, is

$$\phi(\Omega) = \frac{\sigma^2 L}{\pi} \frac{[1 + 2(n+1)b^2(\Omega L)^2]}{[1 + b^2(\Omega L)^2]^{n+3/2}} \quad (4)$$

where  $n$  and  $b$  are constants.

The second family, designated the Taylor-Bullen longitudinal family, is defined by

$$\phi(\Omega) = \frac{2\sigma^2 L}{\pi} \frac{1}{[1 + b^2(\Omega L)^2]^{n+1/2}} \quad (5)$$

The third family, designated the sharp-knee family, is defined by

$$\phi(\Omega) = \frac{\text{Constant}}{1 + (\Omega L)^{-m}} \quad (6)$$

and the fourth family, proposed by Hoblit and designated the mild-knee family, is defined by

$$\phi(\Omega) = \frac{\text{Constant}}{(1 + \Omega L)^{-m}} \quad (7)$$

where the Constant = 
$$\frac{4 \pi L \sigma^2}{3}$$

Figures 12 a-e illustrate the curves defined by Taylor-Bullen, sharp-knee and the mild-knee equations for  $m = -5/3$  and for five values of the scale length,  $L$ . Inspection of these curves and of the equations leads to the following conclusions relating to the interpretation of the HICAT spectra given by Crooks, et al, (1, 2).

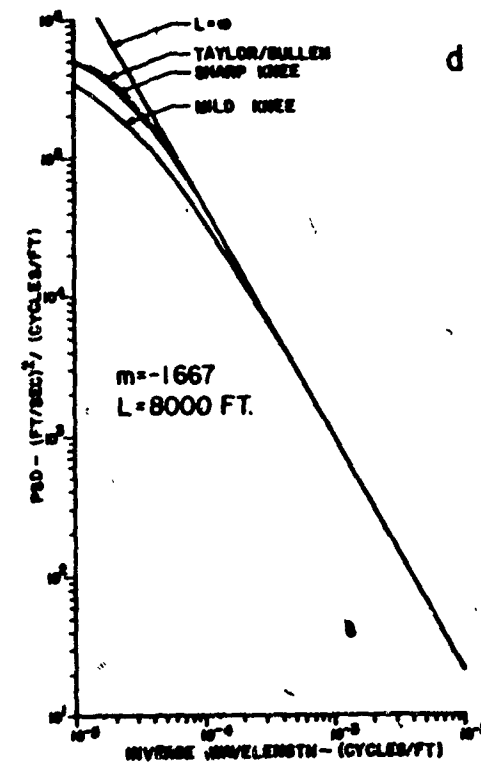
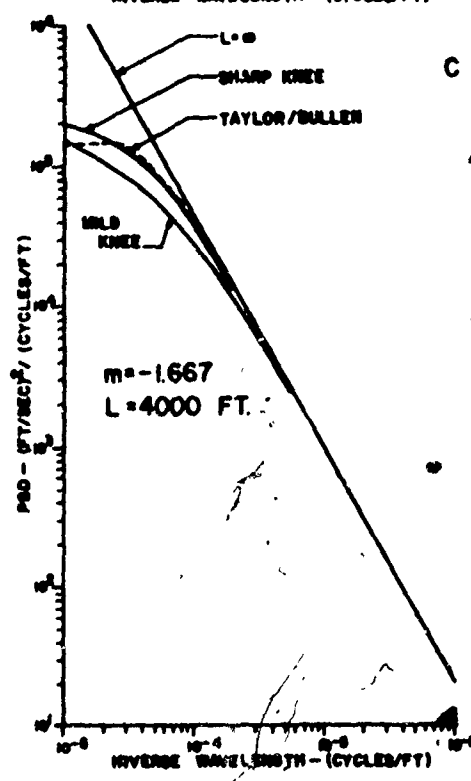
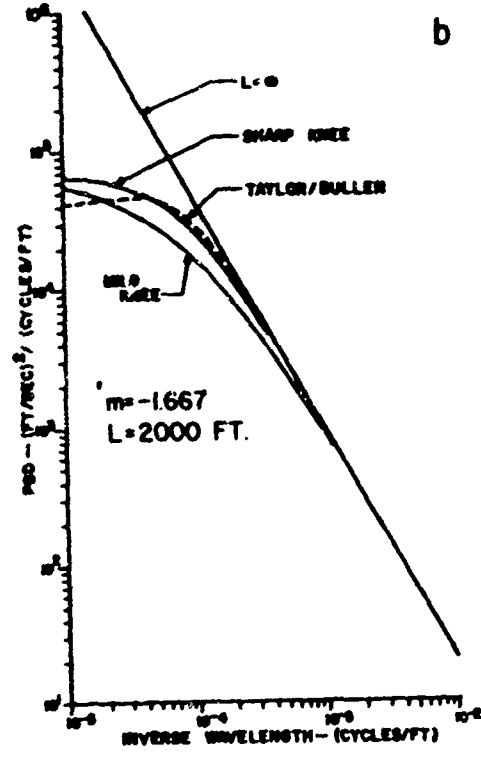
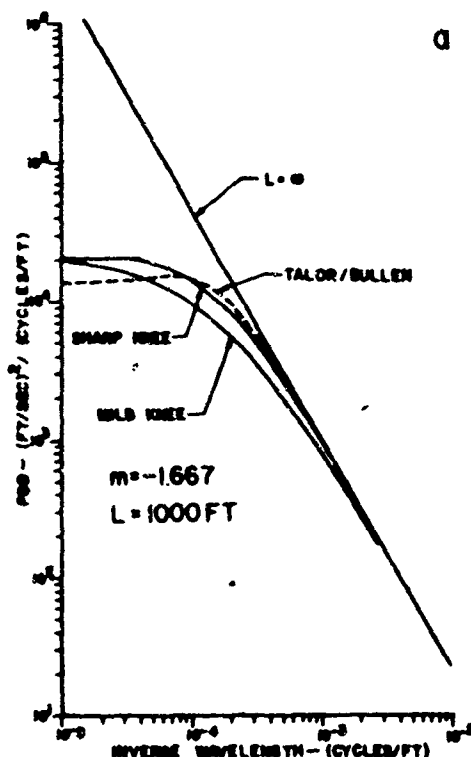
- a) For the case of the low frequency truncation line at  $2.5 \times 10^{-4}$  cycles/ft., there is a significant difference between the equations when  $L < 1,000$  ft. For  $1,000 < L < 4,000$  ft. the "mild-knee" equation differs significantly from the other equations. For  $L > 4,000$  ft. the difference between any two of the equations is insignificant.
- b) For the low frequency truncation line at  $10^{-4}$  cycles/ft., there is a significant difference between the "mild-knee" equation and the other equations for  $L < 8,000$  ft. When  $L > 8,000$  ft. there is no significant difference between the equations.

Crooks et al., (1,2) computed the root-mean-square gust velocities for the low frequency truncation line at  $10^{-3}$ ,  $2.5 \times 10^{-4}$ ,  $10^{-4}$ , and  $5 \times 10^{-5}$  cycles/ft. There were relatively few cases for the truncation line at  $5 \times 10^{-5}$  cycles/ft. If the hypothesis is made that the power spectral density curves are adequately represented by any of the equations listed above and that the slope at the high frequency ( $7.4 \times 10^{-3}$  cycles/ft.) end of the curve is known, then the value of the scale length,  $L$ , can be related to the ratio of  $\text{RMS}(2.5 \times 10^{-4})/\text{RMS}(10^{-3}$  cycles/ft.) and also of  $\text{RMS}(10^{-4}$  cycles/ft.)/ $\text{RMS}(10^{-3}$  cycles/ft.). Tables VII-VIII and Figures 13 and 14 give the values of these ratios for various values of the slope,  $m$ , and scale length,  $L$ . A detailed analysis of the method used to calculate scale lengths from RMS ratios is presented in Appendix I.

Figures 13 and 14 and Table IX indicate that for values of  $m \approx -5/3$ , the difference in the ratios of the root-mean-square gust velocities for scale lengths averaging 2,000 ft. and 4,000 ft., using the mild-knee equation, is relatively large. Consequently, if the mild-knee equation adequately represents the HICAT spectra, then only gross determinations of the scale length can be made.

#### Scale Lengths for the Total HICAT Sample

Scale lengths representative of the total HICAT sample may be obtained by several methods. Crooks, Hoblit, and Mitchell (2) obtained composite spectra by two different methods and then estimated the scale lengths by visually comparing the composite spectra with the curves defined by Equations 4 - 7. The first set of composite spectra were obtained by first preparing cumulative probability curves for the psd values at each of various frequencies. Each



Figures 12 a, b, c, d, e  
 Comparison of Taylor-Bullen, Sharp-Knee and Mild-Knee Equations for  
 Different Values of L

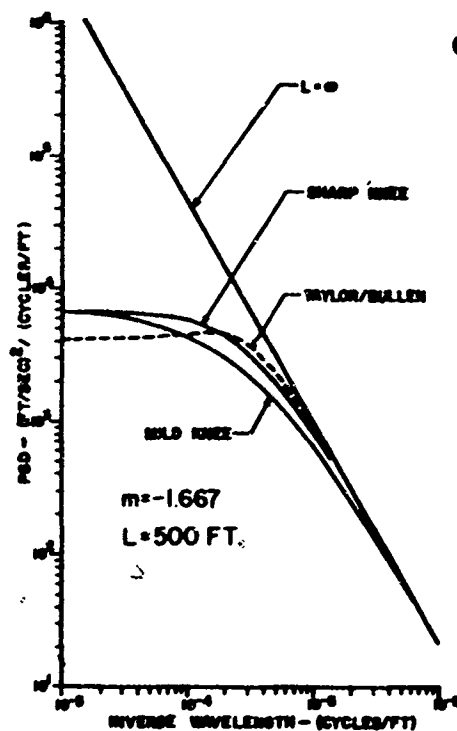


Figure 12 (Cont.)

value was weighted according to the length of the turbulent region. Then probability levels were selected and the pdf values corresponding to these probability levels were plotted as a function of frequency. In this way composite spectra were obtained that represented the 0.5, 0.1 and the 0.01 probabilities, respectively. This method of obtaining composite spectra has the advantage of clearly indicating any differences that might exist in the spectra representing turbulence of different intensities. The second set of composite spectra was defined by the average of the normalized spectra. The results obtained by Crooks, et al., are summarized in Table 10.

TABLE VII. RMS ( $2.5 \times 10^{-4}$  cycles/ft.) / RMS ( $10^{-3}$  cycles/ft.) for the Mild-Knee Equation (Equation 7).

L	m								
	-1.3	-1.4	-1.5	-1.6	-1.67	-1.7	-1.8	-1.9	-2.0
500 ft.	1.303	1.338	1.375	1.416	1.446	1.459	1.506	1.556	1.610
1,000	1.361	1.407	1.457	1.512	1.553	1.571	1.635	1.704	1.779
2,000	1.404	1.458	1.518	1.584	1.634	1.657	1.735	1.821	1.913
3,000	1.421	1.480	1.544	1.615	1.669	1.693	1.778	1.870	1.970
4,000	1.431	1.491	1.558	1.632	1.688	1.713	1.801	1.897	2.002
5,000	1.437	1.499	1.567	1.642	1.670	1.725	1.816	1.915	2.022
6,000	1.441	1.504	1.573	1.650	1.708	1.734	1.826	1.927	2.036
8,000	1.446	1.510	1.581	1.659	1.719	1.745	1.839	1.942	2.055
10,000	1.450	1.514	1.586	1.665	1.725	1.752	1.848	1.952	2.066
15,000	1.454	1.520	1.593	1.673	1.734	1.762	1.859	1.965	2.081



TABLE VIII. RMS ( $10^{-4}$  cycles/ft)/ RMS ( $10^{-3}$  cycles/ft) for the Mild-Knee Equation (Equation 7)

L	m								
	-1.3	-1.4	-1.5	-1.6	-1.67	-1.7	-1.8	-1.9	-2.0
500 ft.	1.414	1.466	1.523	1.586	1.633	1.654	1.729	1.809	1.896
1,000	1.523	1.598	1.683	1.777	1.848	1.880	1.995	2.217	2.259
2,000	1.618	1.716	1.828	1.953	2.050	2.093	2.250	2.425	2.618
3,000	1.662	1.772	1.897	2.039	2.148	2.198	2.377	2.577	2.801
4,000	1.689	1.805	1.939	2.090	2.207	2.261	2.453	2.670	2.913
5,000	1.706	1.827	1.966	2.124	2.246	2.302	2.504	2.718	2.988
6,000	1.718	1.843	1.985	2.148	2.275	2.332	2.541	2.777	3.040
8,000	1.734	1.863	2.011	2.180	2.312	2.372	2.590	2.837	3.115
10,000	1.744	1.876	2.028	2.200	2.336	2.398	2.622	2.875	3.162
15,000	1.759	1.895	2.051	2.230	2.370	2.434	2.667	2.930	3.228

All of the composite spectra obtained from either the cumulative probability procedure or the averaging procedure with the spectra truncation line taken at  $\Omega = 2.5 \times 10^{-4}$  cycles/ft ( $\lambda = 4,000$  ft) indicate an infinite scale length.

The scale lengths may also be determined through the use of the computations given in Tables VII and VIII and Figures 13 and 14 combined with the values of the root-mean-square gust velocities published by Crooks, et al., (1, 2). If the slopes of the average spectra (Table X) are used, scale lengths of 1,200, 6,000 and 3,000 ft. for the vertical, lateral, and longitudinal components, respectively, are indicated. If only the sets of spectra are used for which the vertical component of the RMS ( $5 \times 10^{-4}$  cycles/ft) is equal to or greater than 1.0 ft/sec, then the slopes are found to be as indicated for the 0.5 probability level and the scale lengths are 2,000 ft, 3,000 ft, and  $\infty$  for the vertical, lateral and longitudinal components, respectively.

In Figure 15 composite spectra and their associated scale lengths and slopes obtained by yet another method are presented for the three components of the gust velocity using the total HICAT sample. The composite values were arrived at by (1) averaging the logarithms of the ordinate values at various frequencies and (2) taking the antilog of the averages. The advantage of this method over one which uses direct averages of the ordinates is that the latter, because of distortion due to the logarithm scale, tends to give unequal weight to spectra with less bending at low frequencies whereas composite spectra derived from averaging logarithms more closely resemble the median value.

Scale lengths of over 8,000 feet are obtained by this method of averaging the logarithms of the ordinates. Spectra with root-mean-square gust velocities (truncated at  $5 \times 10^{-4}$  cycles/ft)  $\geq 1.0$  ft/sec and extending to  $10^{-4}$  cycles/ft were used in obtaining the composite spectra.

Figure 16 illustrates the results obtained when the data used to determine the spectra for the vertical component given in Figure 15 are divided into two intensity classes. The composite spectrum representing the high intensity cases has a steeper slope and a shorter scale length than the spectrum for the low intensity cases but the difference appears insignificant.

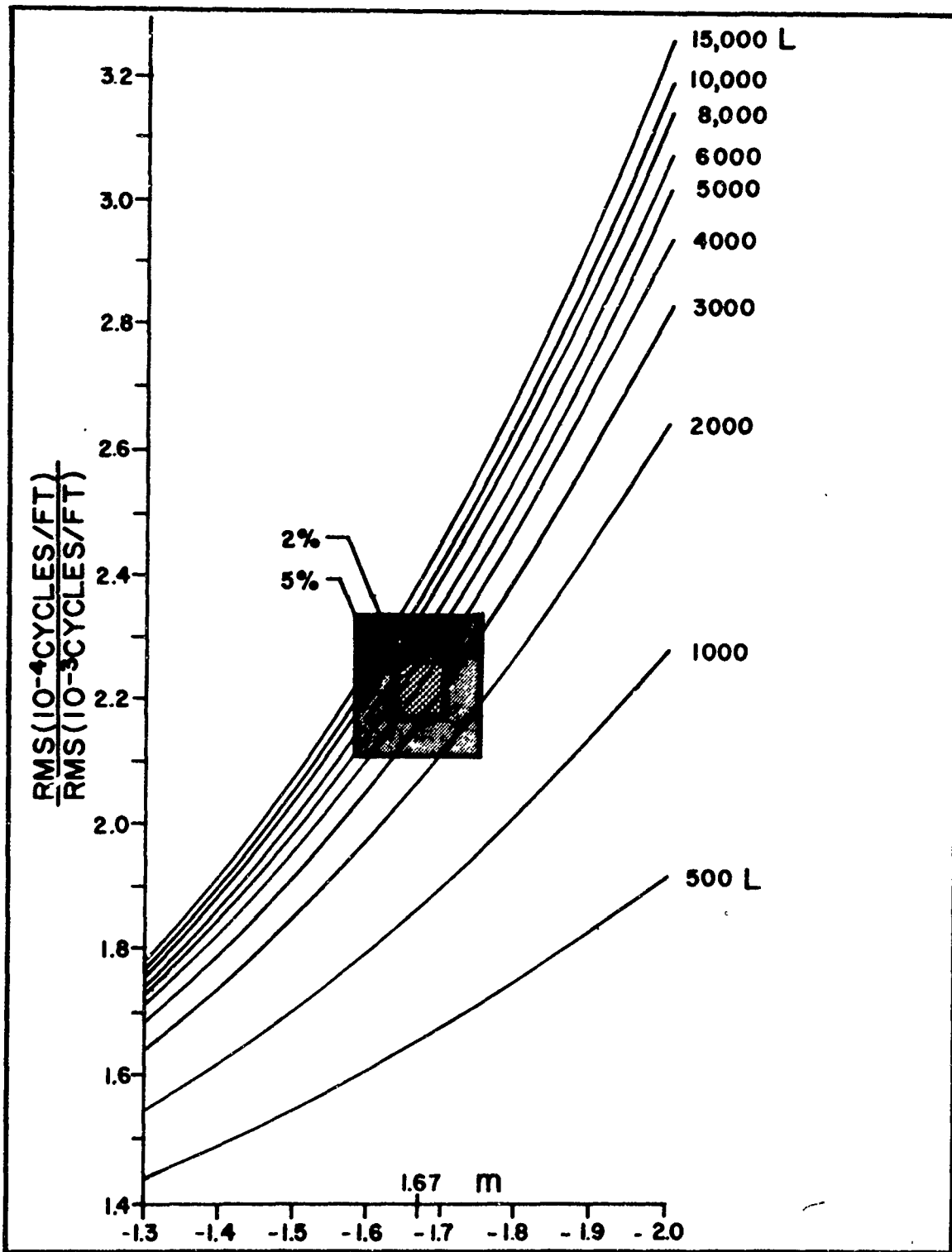


Figure 13. Scale Length,  $L$ , as a Function of the Ratio of Root-Mean-Square Gust Velocities and Slope,  $m$ , for the Mild-Knee Equation. (Shaded Areas Indicate Effects of 2% and 5% Uncertainties in the Abscissa and Ordinate Values)

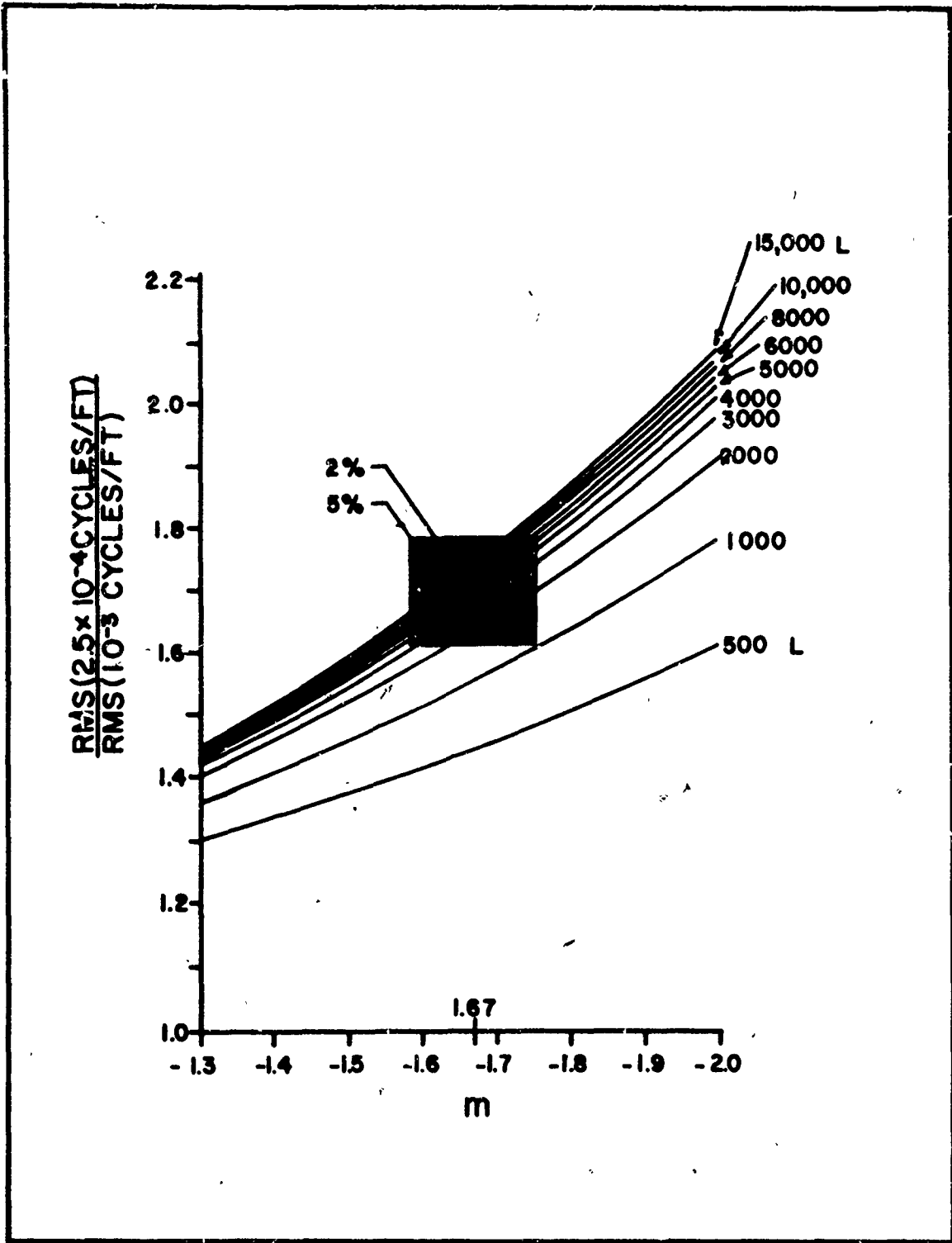


Figure 14. Scale Length, L, as a Function of the Ratio of Root-Mean-Square Gust Velocities and Slope, m, for the Mild-Knee Equation. (Shaded Areas Indicate Effects of 2% and 5% Uncertainties in the Abscissa and Ordinate Values)

TABLE IX. Range in Computed Values of Scale Length for Various Errors in  $m$  and Ratio of the Root-Mean-Square Gust Velocities.

Error in RMS ( $2.5 \times 10^{-4}$ )/RMS ( $10^{-3}$ )	Range in L (Mean L = 2,000 ft)	Range in L (Mean L = 4,000 ft)
$\pm 2\%$ $\pm 5\%$	1700 to 2600 ft 900 to 6000 ft	2800 to 6000 ft 1500 to "
Error in $m$ (Mean $m = -1.67$ ) $\pm 2\%$ $\pm 5\%$	1700 to 2600 ft 1400 to 4500 ft	3000 to 8000 ft 2000 to "
Error in Ratio of RMS Values Combined with error in $m$ $\pm 2\%$ $\pm 5\%$	1500 to 3500 ft 750 to "	2200 to 15000 ft 1000 to "
Error in RMS ( $10^{-4}$ )/RMS ( $10^{-3}$ ) $\pm 2\%$ $\pm 5\%$	1700 to 2500 ft 1400 to 3000 ft	3300 to 5000 ft 2500 to 9000 ft
Error in $m$ (Mean $m = -1.67$ ) $\pm 2\%$ $\pm 5\%$	1700 to 2400 ft 1500 to 3500 ft	3200 to 5600 ft 2500 to 13000 ft
Error in Ratio of RMS Values Combined with error in $m$	1500 to 3000 ft 1100 to 6000 ft	2600 to 7000 ft 1700 to "

TABLE X. Slopes and Scale Lengths of Composite Spectra (Minimum  $\Omega = 10^{-4}$  cycles/ft)  
(Crooks, et al (2) ).

	Slope, m			Scale Length, L		
	Vertical	Lateral	Longitudinal	Vertical	Lateral	Longitudinal
0.5 Probability Level-Sharp-Knee Mild-Knee	-1.64	-1.87	-1.57	2000 ft	1800 ft	4000 ft
	-1.64	-1.87	-1.57	2000	1900	2000
	-1.64	-1.87	-1.57	4000	3500	4000
Taylor-Bullen 0.1 Probability Level-Sharp-Knee Mild-Knee	-1.64	-1.87	-1.57	2000	2000	4000
	-1.64	-1.87	-1.57	2000	1500	2000
	-1.64	-1.87	-1.57	4000	3500	4000
Taylor-Bullen Average Spectra - Sharp-Knee Mild-Knee	-1.71	-1.71	-1.71	>2000	>3000	2000
	-1.71	-1.71	-1.71	>4000	>3000	3000
	-1.71	-1.71	-1.71	>6000	>6000	3000

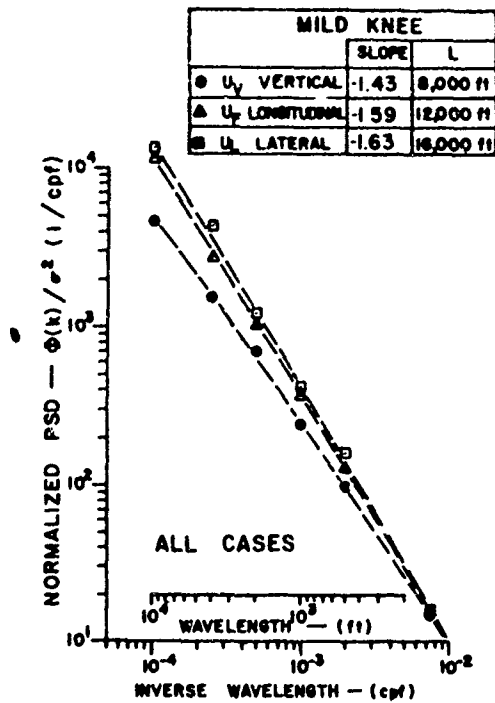


Figure 15. Spectra, Slopes and Scale Lengths for the Total HICAT Sample.

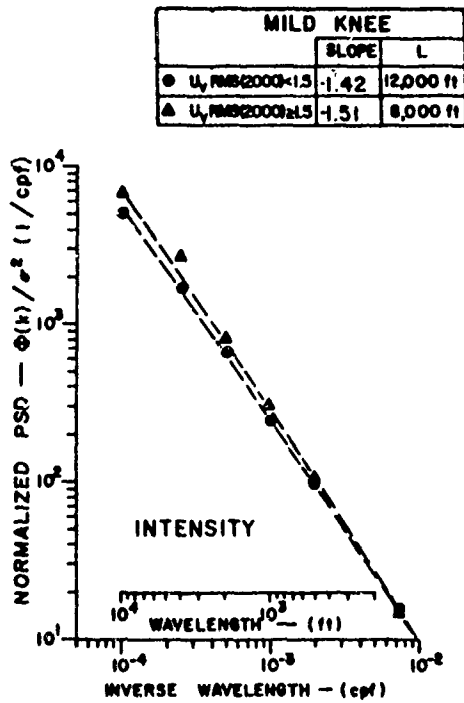


Figure 16. Comparison of Normalized Composite Spectra Separated by Intensity of the Turbulence.

Scale Lengths of Composite Spectra Representing Topographic and Altitude Categories.

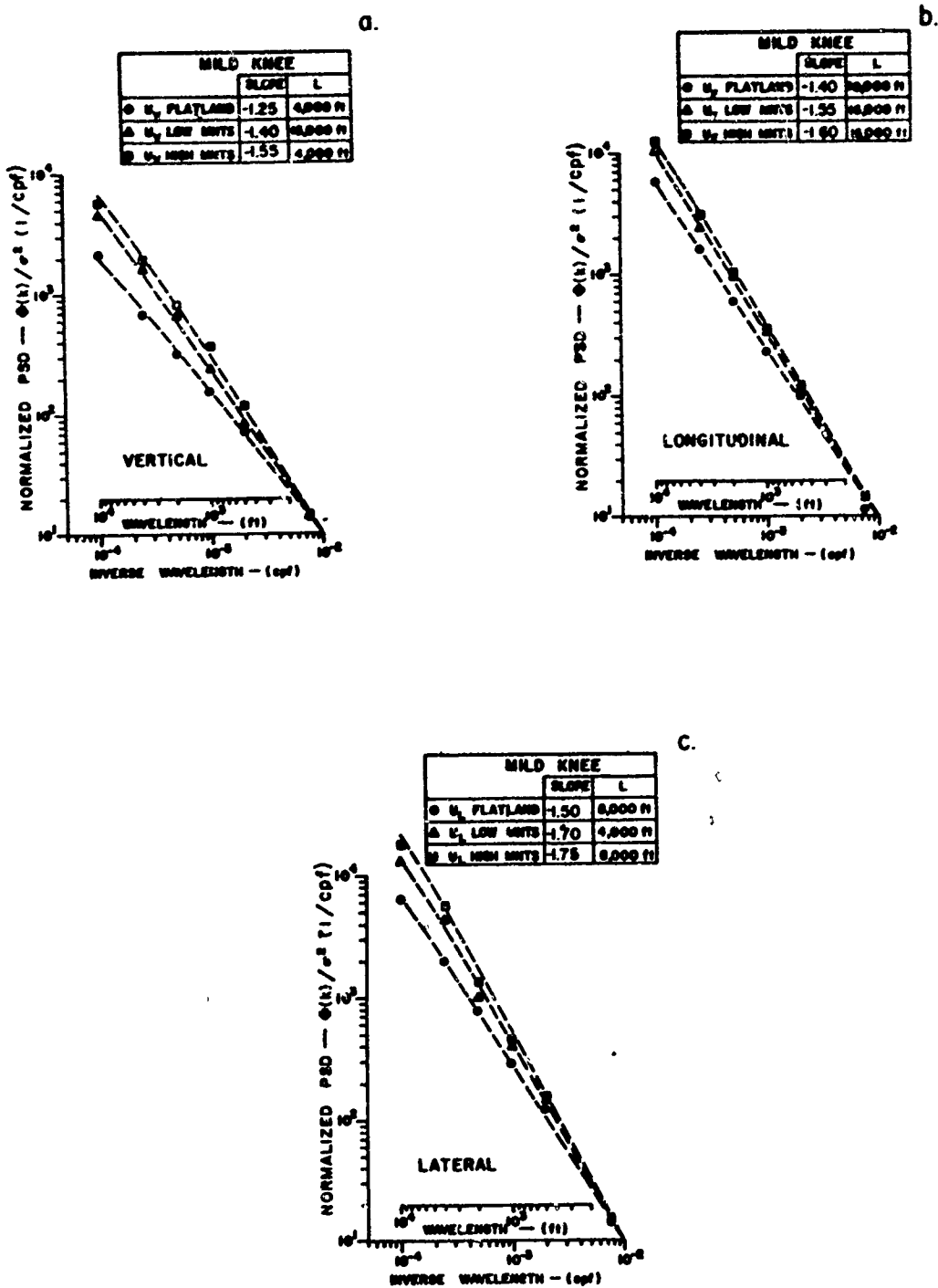
Three methods were used to determine the scale lengths of the composite spectra representing the topographic and altitude categories. The results are presented in Table XI. In the first method the composite spectra were obtained by averaging the logarithms of the individual spectra ordinate values as explained earlier in the section. These spectra are illustrated in Figures 17 and 18. In the second and third methods scale lengths were obtained by comparing calculated values of RMS ( $2.5 \times 10^{-4}$  cycles/ft)/RMS ( $10^{-3}$  cycles/ft) and RMS ( $10^{-4}$  cycles/ft)/RMS ( $10^{-3}$  cycles/ft) with the values for the mild-knee equation listed in Tables VII and VIII. A detailed description of these methods is found in Appendix I.

TABLE XI. Scale Lengths of Composite Spectra

Category	Vertical Component			Lateral Component			Longitudinal Component		
	Figure 17 & 18	Table VII	Table VIII	Figure 17 & 18	Table VII	Table VIII	Figure 17 & 18	Table VII	Table VIII
Altitude < 59,000 Ft	8,000 ft	"	"	16,000	8,000	"	16,000	"	"
Altitude > 59,000 Ft	8,000	"	"	16,000	8,000	"	16,000	"	"
Flatland	4,000	"	4,000	8,000	"	12,000	40,000	"	"
Low Mountains	16,000	"	"	4,000	3,500	5,500	16,000	"	"
High Mountains	4,000	"	15,000	8,000	"	8,000	16,000	"	"

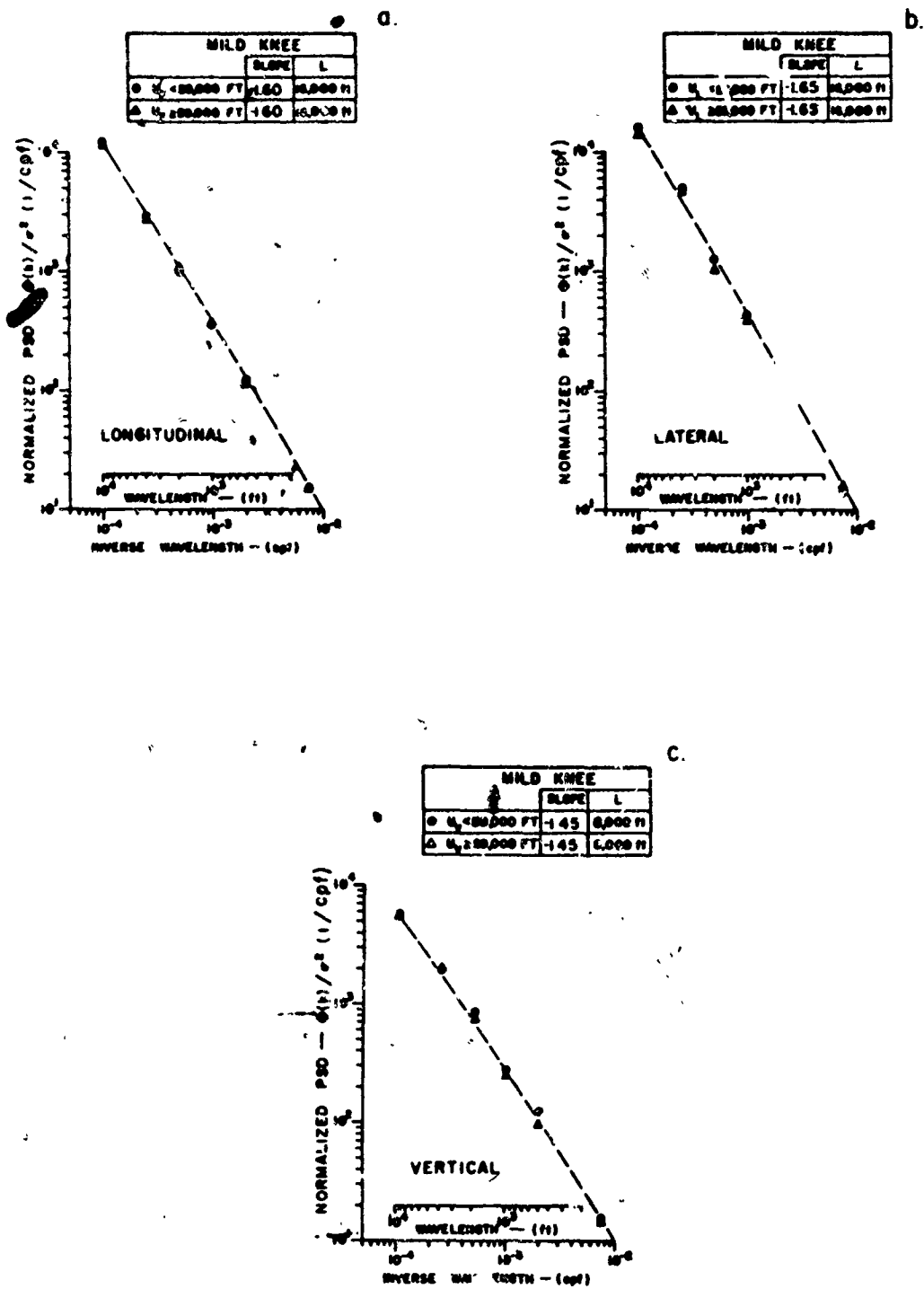
Computations of the scale lengths can be made using the correlation function method described by Houbolt (5). This method requires data which is essentially unfiltered. The data sample available from HICAT records, however, was high-pass filtered and characterized by rapidly decaying correlation functions resulting in scale lengths about one order of magnitude lower than what was derived using other techniques.

In the following section the scale lengths given by the composite spectra (Figures 15 to 18) will be used in converting the root-mean-square gust velocities obtained from the truncated spectra to those useful in aircraft gust load calculations.



Figures 17(a,b,c). Composite Spectra for Topographic Categories





Figures 18 a, b, c. Composite Spectra for Altitude Categories

## SECTION IV

### STANDARD DEVIATION OF THE ROOT-MEAN-SQUARE GUST VELOCITY

#### Introduction

Aircraft gust load calculations are based in part upon the probability density distribution of the root-mean-square gust velocity. This probability density distribution is conventionally defined as the sum of two normal density distributions weighted by  $P_1$  and  $P_2$ ,

$$P(\sigma) = \left( \frac{P_1}{b_1} \right) \sqrt{2/\pi} \exp \left( -\frac{\sigma^2}{2b_1^2} \right) + \left( \frac{P_2}{b_2} \right) \sqrt{2/\pi} \exp \left( -\frac{\sigma^2}{2b_2^2} \right) \quad (8)$$

where  $P_1$  and  $P_2$  are the proportions of total flight time in "non-storm" and "storm" turbulence respectively;  $b_1$  and  $b_2$  are the standard deviations of the root-mean-square gust velocity,  $\sigma_{\pi}$ , in non-storm turbulence and storm turbulence respectively.  $\sigma_{\pi} = \sigma - x$ ;  $\sigma$  is the true root-mean-square gust velocity and  $x$  is the minimum value of  $\sigma$  to be classified as turbulence. The root-mean-square gust velocity is equal to the square root of the area under the complete power spectral density curve. Power spectral density curves computed from measurements have truncation limits that are a function of the length of the turbulence record, instrument capabilities and the computation technique. If the power spectral density curves computed from the gust velocity measurements are found to be adequately represented within the frequency range of the measurements, by an equation (e.g. one of Equations 4 through 7) then this equation may be used to determine the area under the curve with the frequency limits set at 0 and  $\infty$ , providing an assumption is made that the equation adequately represents the spectra at frequencies outside the range of the measurements.

This assumption suggests the following example. Consider, two observations of turbulence with equal root-mean-square gust velocities computed from spectra truncated at  $5 \times 10^{-4}$  cycles/ft. ( $\lambda = 2,000$  ft). In one case the turbulence region is just long enough to compute the spectrum out to this truncation limit. In the second case the turbulence region is long enough to provide a spectrum to a truncation limit of  $10^{-5}$  cycles/ft. ( $\lambda = 10,000$  ft). Suppose that the two spectra have the same slope and curvature up to  $5 \times 10^{-4}$  cycles/ft. ( $\lambda = 2,000$  ft) and hence can be represented by the same equation within the common frequency range. In such a circumstance the physical situation in the turbulent region from which the shorter record was obtained is assumed identical to that of the longer record which is, of course, not necessarily so. However, for purposes of this section the assumption is considered valid.

### Estimating $b_1$ 's

In Section II the probability density distributions were determined for the measured root-mean-square gust velocities obtained from the spectra between the truncation limits  $7.4 \times 10^{-3}$  and  $5 \times 10^{-4}$  cycles/ft. These probability density distributions were converted into probability density distributions of  $\sigma_T$  through use of the following procedure:

- a) The "mild-knee" equation (Equation 7, Section III) was assumed to best represent all the power spectral density curves. It should be noted, however, that for L's on the order of those derived from the HICAT spectra (8,000 - 16,000 ft) the choice of equations has only a small effect on the results.
- b) The values of scale length, L, and slope, m, given for the various composite spectra discussed in Section III were applied to the individual spectra. Consequently, the individual spectra were assumed to differ from each other only in the "scale factor" that indicates the relative intensity of the turbulence.
- c) Table XII was used to convert the root-mean-square gust velocities obtained from the truncated spectra to the root-mean-square gust velocities obtained from Equation 7 between the limits 0 and  $\infty$  cycles/ft.

The justification for the assumption made in (a) was that those spectra obtained from the long turbulent regions were best represented by the "mild-knee" equation. As the discussion in Section III indicated, no definite choice between Equations 4 through 7 could be made for the spectra obtained from the relatively short turbulent regions.

The justification of the assumption made in (b) was that the scale of turbulence, L, could not be determined for the spectra with the truncation at  $5 \times 10^{-4}$  cycles/ft. and hence values for L had to be assumed. The L's given by the composite spectra appeared to be the most reasonable. The slopes of the composite spectra were used so as to be consistent with the scale lengths.

The standard errors of the  $b_1$ 's listed in Table XIII are estimated to be at least 50% of the values listed. The uncertainties in the values of the  $b_1$ 's arise principally because power spectral density curves computed from the gust velocity measurements cover a relatively limited frequency range. Errors on the evaluation of the  $b_1$ 's arise because

- a) The values of s, (standard deviation of RMS ( $\lambda = 2,000$  ft)) may vary as much as 50% as the definition of the lower boundary of turbulence is changed over reasonable limits. In the preparation of Table XIII turbulence was defined to exist if  $U_v (5 \times 10^{-4} \text{ cycles/ft}) \geq 0.5 \text{ ft/sec}$ .

TABLE XII

Ratio of  $\sigma_T$  to Root-Mean-Square Gust Velocity  
 From Spectra Truncated at  $5 \times 10^{-4}$  Cycles/Ft (Based on Mild-Knee Equation)

L	m								
	1.3	1.4	1.5	1.6	1.67	1.7	1.8	1.9	2.0
500 Ft	1.29	1.33	1.38	1.43	1.46	1.48	1.54	1.60	1.66
1,000	1.42	1.49	1.57	1.66	1.73	1.76	1.86	1.98	2.11
2,000	1.59	1.70	1.83	1.98	2.10	2.15	2.34	2.55	2.80
3,000	1.70	1.85	2.02	2.21	2.37	2.44	2.70	3.00	3.35
4,000	1.78	1.96	2.16	2.40	2.59	2.68	3.07	3.38	3.82
5,000	1.85	2.05	2.28	2.56	2.78	2.89	3.27	3.71	4.23
6,000	1.91	2.13	2.39	2.70	2.95	3.01	3.50	4.01	4.62
8,000	2.00	2.26	2.57	2.94	3.24	3.38	3.92	4.55	5.30
10,000	2.08	2.37	2.72	3.14	3.49	3.65	4.27	5.01	5.90
15,000	2.23	2.58	3.00	3.54	3.99	4.20	5.00	5.99	7.18

TABLE XIII

Values of  $s$ ,  $L$ ,  $m$ ,  $b_1$  and  $\bar{x}$  For High Altitude Clear Air Turbulence

Category	$s$ (ft/sec)			$L$ (ft)			$m$			$b_1$ (ft/sec)			$\bar{x}$ (ft/sec)		
	Vert.	Lat.	Long.	Vert.	Lat.	Long.	Vert.	Lat.	Long.	Vert.	Lat.	Long.	Vert.	Lat.	Long.
Water	0.46	0.50	0.41	8,000	8,000	16,000	-1.25	-1.50	-1.45	0.9	1.5	1.2	0.95	2.23	2.41
Flatland	0.61	0.79	0.54	8,000	8,000	16,000	-1.25	-1.50	-1.45	1.2	2.0	1.5	0.95	2.21	2.18
Low Mountains	0.86	1.00	0.92	8,000	8,000	16,000	-1.40	-1.70	-1.55	1.9	3.4	3.1	1.11	2.64	2.48
High Mountains	1.25	1.27	1.27	8,000	8,000	16,000	-1.55	-1.75	-1.60	3.4	4.6	4.6	1.37	2.92	2.88
45,000 - 49,900 ft	0.61	0.69	0.48	8,000	8,000	16,000	-1.45	-1.65	-1.55	1.5	2.2	1.6	1.20	2.81	2.74
50,000 - 54,900 ft	0.96	1.03	0.93	8,000	8,000	16,000	-1.45	-1.65	-1.55	2.3	3.3	3.1	1.20	2.94	2.61
55,000 - 59,900 ft	0.90	0.83	0.83	8,000	8,000	16,000	-1.45	-1.65	-1.55	2.2	2.6	2.8	1.20	2.56	2.34
$\geq 60,000$ ft	1.09	1.20	1.19	8,000	8,000	16,000	-1.45	-1.65	-1.55	2.6	3.8	4.0	1.20	2.37	2.34
All Cases	0.94	0.96	0.91	8,000	8,000	16,000	-1.45	-1.65	-1.55	2.3	3.0	3.0	1.20	2.72	2.48

- b) The scale length,  $L$ , can only be crudely estimated for the spectra obtained from short records. Here it was assumed that these spectra have the same distribution of  $L$ 's as the spectra from long records.
- c) Various methods of determining composite spectra yield different values of  $L$  and  $m$ . The values given in Table XIII are considered a best estimate.

If the definition of the lower limit of turbulence that is given in (a) is accepted then the lower limit of  $\sigma_T$  for turbulence becomes a function of  $L$  and  $m$ . These lower limits,  $\bar{x}$  (see Equation 8), are also listed in Table XIII. In Section V the lower limit of turbulence used to define the ratio of turbulent flight miles to total flight miles is defined in terms of the cg normal acceleration, where frequently occurring peaks of  $\pm 0.10g$  are equated to a  $U_v$  RMS ( $\lambda = 2,000$  ft) of 0.5 ft/sec.

## SECTION V

### RATIO OF TURBULENT FLIGHT MILES TO TOTAL FLIGHT MILES

#### Definition of Turbulence

When an aircraft that is flying through a portion of the atmosphere in which there are no clouds undergoes accelerations that cannot be directly attributable to the movement or setting of the control surfaces, the aircraft is said to be in clear air turbulence. The accelerations of the aircraft are functions of the weight and characteristics of the aircraft in addition to the atmospheric gusts. If the ratio of the turbulent flight miles to the total flight miles is to be computed, definitions of turbulent and total flight miles are required. The definition of the turbulent flight miles must include statements that give (1), the lower limit of accelerations that are considered to be turbulence, (2), the frequency interval of interest, and (3), a quantitative evaluation of the duration of the turbulence. If the turbulent regions are not randomly distributed in space and time, the ratio of turbulent flight miles to total flight miles is also a function of, (1), the distribution and total number of flight miles by altitude, season, and topographic region, (2), turbulence search or avoidance procedures, if successful, and (3), pattern flying through a known turbulent region.

In Section II, for the purpose of determining the probability density distribution of the vertical component root-mean-square gust velocity, turbulence was defined to exist when  $U_{\text{RMS}}$  ( $\lambda = 2,000$  ft) was equal to or greater than 0.5 ft/sec. This definition of clear air turbulence is in apparent conflict with the definition given in terms of the aircraft acceleration. For the purpose of determining the ratio of the turbulent flight miles to the total flight miles, the definition of turbulence given below in terms of acceleration of the aircraft was used because the gust data were incomplete from the HICAT flight program and non-existent from the NASA U-2 flight program. In addition, the turbulent region had to be approximately 8 miles long to provide adequate data for a spectra of minimum usable length. Thus, if the RMS gust velocity was used to define turbulence, all turbulent regions shorter than 8 miles would be ignored.

In his review of the VGH data from 768,000 miles in the altitude range 40,000 to 70,000 ft. of NASA U-2 flights Steiner ( 5 ) defined turbulence to exist "whenever the accelerometer trace was disturbed and contained gust velocities (presumably "derived" gust velocities,  $U_{\text{de}}$ ) greater than 2 ft/sec." Crooks (1) defined turbulence to exist whenever the  $cg$  normal acceleration trace showed frequently occurring peaks of  $\pm 0.10$  g. The beginnings and endings of turbulence were given to the nearest 5 seconds and turbulence of less than ten seconds duration was counted as no turbulence. A comparison of the maximum  $U_{\text{de}}$  values of the HICAT and the NASA flights indicates that Crooks' and Steiner's criteria for turbulence are approximately equivalent.

The classification of the HICAT turbulence and non-turbulence flight miles

by altitude, underlying topography and by season was done subjectively. The principal difficulty was associated with patterns or repeated flights through a region that was found to be turbulent on the flight through the region. In general, the turbulence was found to vary in intensity and duration for each flight through the region. Approximately 345,000 flight miles of the more than 500,000 flight miles were used in the determination of the ratio of turbulent flight miles to total flight miles. The 155,000 miles not used were associated with pattern flights, test flights and instrument failure.

Ratio of Turbulent Flight Miles to Total Flight Miles for Categories of Altitude, Topography and Season.

Table XIV lists the estimated ratio for the HICAT flights of the turbulent flight miles to the total flight miles for categories of altitude, topography and season. The topographic categories were defined as follows:

- a) Flatland - relief differences less than 3,000 ft
- b) Low Mountains - relief differences 3,000 to 7,000 ft
- c) High Mountains - relief differences over 7,000 ft.

Turbulence was presumed to exist if the cg acceleration trace frequently exceeded  $+0.10g$ . Table XV compares the ratios given by Steiner (5) for the NASA U-2 flights, the HICAT program and by MIL-A-8861A for altitude intervals. Table XVII lists the ratios of the turbulent flight miles to total flight miles that are recommended by the authors for use in the design and operation of advanced aircraft. The ratios obtained from an analysis of the HICAT data were judged to be high mainly because of the search procedures used. The NASA flights were probably distributed more nearly to the expected flight operations. This also justified lowering the ratios obtained from HICAT data.

The proportion of the total flight miles that are turbulent varies significantly with the definition of turbulence. The relative magnitude of this variation is illustrated in Table XVII. This table also clearly indicates that there is little change of the relative frequency of occurrence of turbulence with altitude over mountains and a relatively large change with altitude over flatland and water.

The numbers of HICAT flight miles by season and topography are shown in Table XVIII. Flights over mountains were predominantly made in the winter. Flight miles were approximately equally distributed by season over flatland and water. Table XIX indicates the proportion of the total flight miles that were turbulent in categories of season and topography. There was relatively little turbulence during summer and autumn over water and flatland.



TABLE XIV

## Ratio of Turbulent Flight Miles to Total Flight Miles

Category	Total Flight Miles	Ratio Turbulent
65,000 - 69,900 ft	16,000 miles	0.015
60,000 - 64,900	87,000	0.014
55,000 - 59,900	107,000	0.028
50,000 - 54,900	105,000	0.047
45,000 - 49,900	30,000	0.042
45,000 - 69,900	345,000	0.031
Water	124,000	0.027
Flatland	132,000	0.027
Low Mountains	49,000	0.036
High Mountains	40,000	0.049
Winter (Dec. - Feb.)	108,000	0.038
Spring (Mar. - May )	81,000	0.039
Summer (Jun. - Aug.)	71,000	0.019
Autumn (Sept. - Nov.)	85,000	0.024

TABLE XV

Comparison of Steiner (NASA U-2), HICAT and MIL-A-8861A Data

Altitude Interval	Steiner ( )		HICAT		MIL-A-8861A (1968) Ratio Turbulent
	Flight Miles	Ratio Turbulent	Flight Miles	Ratio Turbulent	
60,000-70,000 Ft	576,000	0.006	103,000	0.015	0.001
50,000-60,000 Ft	141,700	0.020	212,000	0.035	0.002
40,000-50,000 Ft	49,500	0.025	30,000	0.042	0.005
40,000-70,000 Ft	768,100	0.009	345,000	0.031	-

TABLE XVI

Recommended Ratios of Turbulent Flight Miles to Total Flight Miles

Category	Ratio Turbulent
65,000-70,000 Ft	0.010
60,000-65,000	0.010
55,000-60,000	0.020
50,000-55,000	0.030
45,000-50,000	0.030
45,000-70,000	0.020
Water	0.018
Flatland	0.018
Low Mountains	0.022
High Mountains	0.030
Winter	0.024
Spring	0.024
Summer	0.014
Autumn	0.018

TABLE XVII

Number of Occurrences by Terrain of Turbulence with Vertical RMS  
Greater than Listed Values for Given Altitude Bands

U <sub>v</sub> RMS (λ = 2,000 ft)	Water, Flatland (100 Samples) Altitude Band			Mountains (120 Samples) Altitude Band		
	<55K	55-60K	>60K ft	<55K	55-60K	>60Kft
>0.5 ft/sec	68	28	4	32	35	33
>1.0 ft/sec	16	6	0	20	20	25
>1.5 ft/sec	4	4	0	13	10	15
>2.0 ft/sec	2	1	0	10	5	7
>2.5 ft/sec	1	0	0	7	2	2

TABLE XVIII

Flight Miles by Season for Four Terrain Types (HICAT Flights 54 to 285)

	Winter	Spring	Summer	Fall	All Seasons
Water	24,950	35,880	37,670	25,390	123,890
Flatland	28,740	34,860	21,700	46,880	132,180
Low Mountains	31,330	5,580	4,870	7,240	49,020
High Mountains	22,390	5,600	6,370	5,280	39,640
All Terrain	107,410	81,920	70,610	84,790	344,730

TABLE XIX

Percentage Flight Miles with Turbulence > Light (cg peaks > +0.10g) and Moderate in  
Parenthesis (cg peaks > + 0.25g) by Season for Four Terrain Types (HICAT Flights 54 to 285)

	Winter	Spring	Summer	Fall	All Seasons
Water	3.4(1.2)	3.7(0.4)	1.7(0.2)	1.9(0.3)	2.7(0.5)
Flatland	3.5(0.8)	3.6(0.9)	1.2(0.1)	2.2(0.1)	2.7(0.5)
Low Mountains	4.3(2.4)	2.9(0.4)	0.8(0.7)	3.5(0.6)	3.6(1.7)
High Mountains	4.1(2.1)	6.9(1.4)	6.6(1.5)	4.7(1.1)	4.9(1.8)
All Terrain	3.8(1.6)	3.9(0.7)	1.9(0.3)	2.4(0.3)	3.1(0.8)

SECTION VI

TURBULENCE ABOVE THUNDERSTORMS

Clear Air Turbulence Above Thunderstorms in the HICAT Program

In the HICAT flight program nearly one tenth of all the clear air turbulence observed during the periods that the aircraft was flying over water or flatland areas was associated with flights above thunderstorms. During the flight program the pilots definitely identified 42 cases of flights above thunderstorms. Turbulence was observed on 41 of these occasions. Table XX lists some of the characteristics of the turbulence.

TABLE XX

Characteristics of Turbulence Above Thunderstorms

Estimated Altitude Above Thunderstorm	Number of Cases	Mean Length of Turbulent Region	$U_{de}$ (Mean Max.)	Mean RMS $U_{de}$
1,000 - 3,000 ft	16	22 nm	7.0 ft/sec	1.60 ft/sec
4,000 - 5,000 ft	13	17	4.9	0.92
6,000 - 9,000 ft	12	10	2.5	0.76
> 9,000 ft	1	0	-	-

The mean length of the turbulent region for those cases of flights 1,000 to 3,000 ft. above thunderstorms is approximately 30% larger than the estimates found in the literature of the mean diameter of thunderstorms. This agreement is considered to be relatively good when the variability of the size of thunderstorms and the small HICAT sample are considered. Data relating to the true gust velocities are not given in Table XX because true gust velocities were only given in four cases. In general, the turbulent regions were not long enough to provide the data needed for the power spectral density computations over a useful frequency range. The decrease in the length of the turbulent regions and in the intensity of the turbulence as indicated by the derived gust velocity,  $U_{de}$ , with increasing altitude above the thunderstorm appears reasonable although the results may be fortuitous because of the small sample.

TABLE XVII

Number of Occurrences by Terrain of Turbulence with Vertical RMS  
Greater than Listed Values for Given Altitude Bands

U <sub>v</sub> RMS (λ = 2,000 ft)	Water, Flatland (100 Samples) Altitude Band			Mountains (120 Samples) Altitude Band		
	<55K	55-60K	>60K ft	<55K	55-60K	>60Kft
>0.5 ft/sec	68	28	4	32	35	33
>1.0 ft/sec	16	6	0	20	20	25
>1.5 ft/sec	4	4	0	13	10	15
>2.0 ft/sec	2	1	0	10	5	7
>2.5 ft/sec	1	0	0	7	2	2

TABLE XVIII

Flight Miles by Season for Four Terrain Types (HICAT Flights 54 to 285)

	Winter	Spring	Summer	Fall	All Seasons
Water	24,950	35,880	37,670	25,390	123,890
Flatland	28,740	34,860	21,700	46,880	132,180
Low Mountains	31,330	5,580	4,870	7,240	49,020
High Mountains	22,390	5,600	6,370	5,280	39,640
All Terrain	107,410	81,920	70,610	84,790	344,730

TABLE XIX

Percentage Flight Miles with Turbulence ≥ Light (cg peaks ≥ +0.10g) and Moderate in  
Parenthesis (cg peaks ≥ +0.25g) by Season for Four Terrain Types (HICAT Flights 54 to 285)

	Winter	Spring	Summer	Fall	All Seasons
Water	3.4(1.2)	3.7(0.4)	1.7(0.2)	1.9(0.3)	2.7(0.5)
Flatland	3.5(0.8)	3.6(0.9)	1.2(0.1)	2.2(0.1)	2.7(0.5)
Low Mountains	4.3(2.4)	2.9(0.4)	0.8(0.7)	3.5(0.6)	3.6(1.7)
High Mountains	4.1(2.1)	6.9(1.4)	6.6(1.5)	4.7(1.1)	4.9(1.8)
All Terrain	3.8(1.6)	3.9(0.7)	1.9(0.3)	2.4(0.3)	3.1(0.8)

## SECTION VI

### TURBULENCE ABOVE THUNDERSTORMS

#### Clear Air Turbulence Above Thunderstorms in the HICAT Program

In the HICAT flight program nearly one tenth of all the clear air turbulence observed during the periods that the aircraft was flying over water or flat-land areas was associated with flights above thunderstorms. During the flight program the pilots definitely identified 42 cases of flights above thunderstorms. Turbulence was observed on 41 of these occasions. Table XX lists some of the characteristics of the turbulence.

TABLE XX

Characteristics of Turbulence Above Thunderstorms

Estimated Altitude Above Thunderstorm	Number of Cases	Mean Length of Turbulent Region	$U_{de}$ (Mean Max.)	Mean RMS $U_{de}$
1,000 - 3,000 ft	16	22 nm	7.0 ft/sec	1.60 ft/sec
4,000 - 5,000 ft	13	17	4.9	0.92
6,000 - 9,000 ft	12	10	2.5	0.76
> 9,000 ft	1	0	-	-

The mean length of the turbulent region for those cases of flights 1,000 to 3,000 ft. above thunderstorms is approximately 30% larger than the estimates found in the literature of the mean diameter of thunderstorms. This agreement is considered to be relatively good when the variability of the size of thunderstorms and the small HICAT sample are considered. Data relating to the true gust velocities are not given in Table XX because true gust velocities were only given in four cases. In general, the turbulent regions were not long enough to provide the data needed for the power spectral density computations over a useful frequency range. The decrease in the length of the turbulent regions and in the intensity of the turbulence as indicated by the derived gust velocity,  $U_{de}$ , with increasing altitude above the thunderstorm appears reasonable although the results may be fortuitous because of the small sample.

The relative frequency of flights above thunderstorms in the PACAT program may be high because of the turbulence seeking flight program and because the bases and time of operation were deliberately chosen to provide flights in areas of high thunderstorm incidence. Thunderstorms are, however, difficult to identify from above in the daytime and hence, the aircraft may have been above thunderstorms on occasions when the pilots were unable to identify the underlying clouds as thunderstorms. Also, the HICAT program lacked a consistent format for pilots reporting thunderstorms when in smooth flight.

Clear air turbulence was observed in the stratosphere at times when there were no thunderstorms below the aircraft. This suggests that clear air turbulence observed above thunderstorms is not necessarily directly physically related to the existence of a thunderstorm below. The record of 41 observations of turbulence out of 42 reports of thunderstorms below the aircraft suggests that the turbulence and the thunderstorm activity is significantly related.

#### World-Wide Distribution of Thunderstorms

Thunderstorms are relatively easily identified in a qualitative sense but a quantitative definition is difficult to devise. Dennis (7) defined a thunderstorm as a shower complex in which there are one or more cells producing lightning and within which the edge-to-edge cell separation does not exceed 30 km (19 miles). Some areas of the world have thunderstorms consisting of only one cell while other parts of the world have squall lines with many cells and extending to several hundreds of kilometers in length. The cells in a given cloud mass may be in different stages of development. One cell may be near the end of its life cycle at the time a new cell is starting to grow rapidly. The duration of thunderstorms is also variable. Prophet (8) has shown that the duration increases with increasing size of the radar echo area of the thunderstorm. For our present purposes, Brooks' (9) estimate of the average duration as one hour will be accepted.

The world-wide distribution of thunderstorms has been given by Brooks (9), World Meteorological Organization (10), and the Handbook of Geophysics (11) in terms of "thunderstorm days". A thunderstorm day is defined as a local calendar day on which thunder is heard. Schonland (12) estimated that one out of seven thunderstorm days have more than one thunderstorm within audible distance. In this report it will be assumed that one out of seven thunderstorm days has two thunderstorms.

The literature relating to the thunderstorms contains a number of estimates of the average size of thunderstorms and of the area seen by one observer. The estimates of these two areas are usually so nearly equal that in this report they will be assumed to be equal. To determine the relative proportion of the total area of a region that is covered by thunderstorms it is not necessary to know the numerical value of the area of the thunderstorms because, if  $n$  is the number of thunderstorm days for a given period of time, then, for any mean area of the thunderstorm, the ratio,  $F$ , of the

area of the world where thunderstorms occur to the total area is given by

$$A = \frac{C}{7} \tau_1 \quad (10)$$

where  $\tau_1$  = time interval for a  
duration of thunderstorm

The fraction  $C/7$  is the correction associated with the one day in seven that has two thunderstorms.

In deriving Equation 10 the assumption was made that the thunderstorm activity is uniformly distributed throughout the day. Allowance for the diurnal variation in thunderstorm activity can be made by multiplying the righthand side of Equation 10 by a correction factor obtained from Figure 9 - 17 in the Handbook of Geophysics (11). This correction factor varies from approximately 0.15 at sunrise to approximately 2.0 in mid-afternoon.

In the areas of the world that have maximum thunderstorm activity, n = 20/month. The value of  $r = 0.06$  for mid-afternoon. According to the data presented by Long (12) on the penetrations of the tropopause by thunderstorms approximately 0.01 of the thunderstorms in the United States exceed 50,000 ft in altitude. This, combined with  $r = 0.06$ , indicates that approximately 0.0006 of the area of a given thunderstorm is in the stratosphere by thunderstorm clouds exceeding 50,000 ft. This value (0.0006) is small compared to the penetration of time in turbulence given in Section 5. Further, these tall thunderstorms may be seen for great distances and can usually be easily avoided. Hence, for the present, the evidence indicates that clear air turbulence above thunderstorms is real but thunderstorm penetration into the stratosphere is infrequent enough to justify not categorizing thunderstorm turbulence in a separate class.



## Section VII

### WORLD-WIDE DISTRIBUTION OF TOPOGRAPHIC CATEGORIES

In Sections II, III, and V data were presented that support the hypothesis that the underlying topography has a significant effect upon the probability density of the RMS gust velocity, the scale length, and the proportion of time in turbulence for the altitude interval under consideration (45,000 to 65,000 ft.). The categories of topography were defined in terms of differences in elevation and not of elevation. Figures 19 to 26 show the world-wide distribution of these topographic categories. Note that there is a significant difference between these maps and maps that indicate altitude only. Plateaus are shown as flatland even though they may be at a relatively great elevation.

The effects of mountain ridges may extend to as much as 50 miles leeward depending upon the wind speed and direction and upon the stability of the atmosphere.

The distribution of the earth's surface area in terms of topographic categories is as follows:

Water	71%
Flatland	23%
Low Mountains	3%
High Mountains	3%

In the HICAT flights approximately 26% of the flight miles were flown above mountains, a figure substantially greater than the 6% of the earth's surface area in this category. It appears that the proportion of time in turbulence expected from several flights randomly distributed throughout the world would be less than the figures recommended in Section V, Table XVI, for the altitude and season categories.

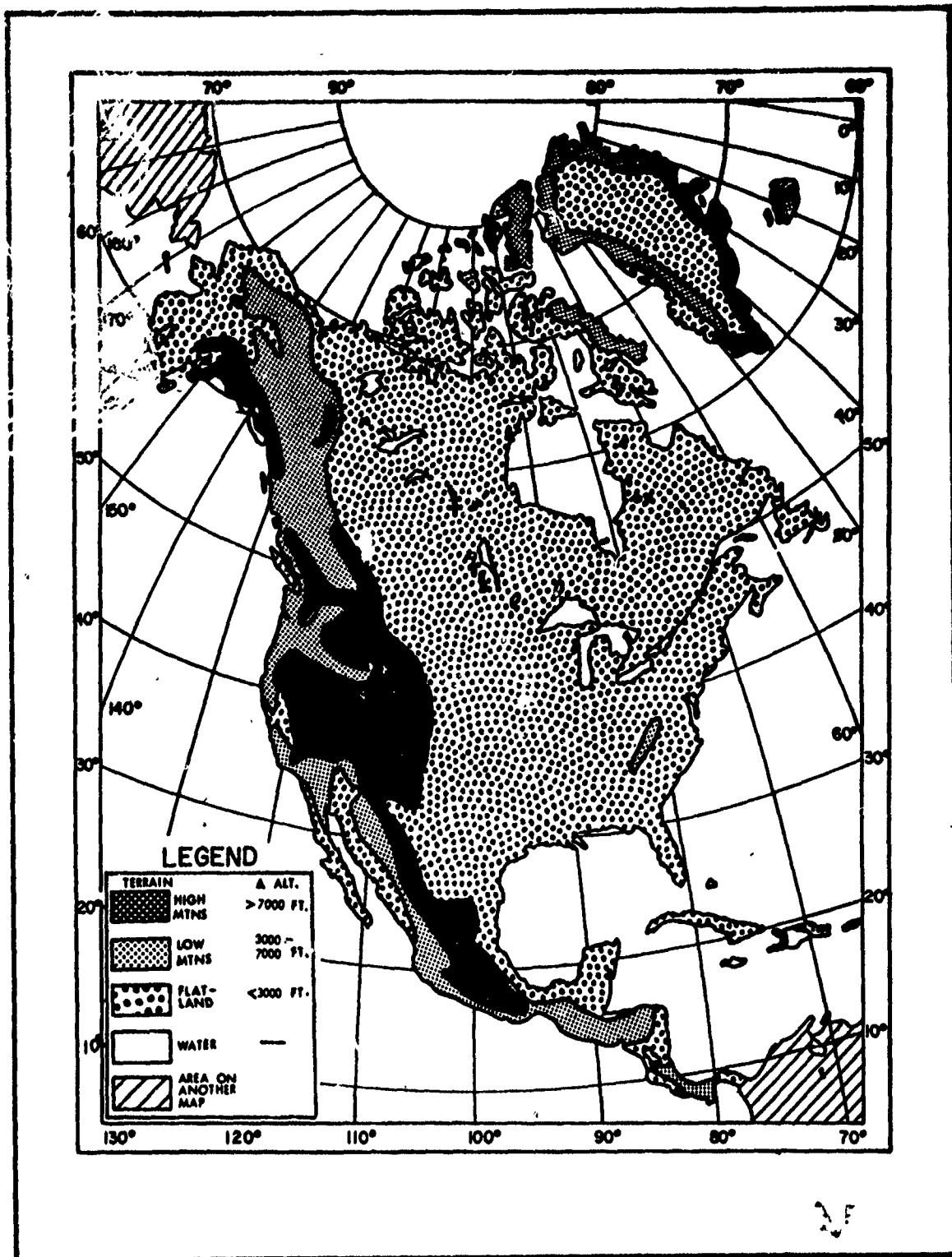


Figure 19. North America - Relief Differences

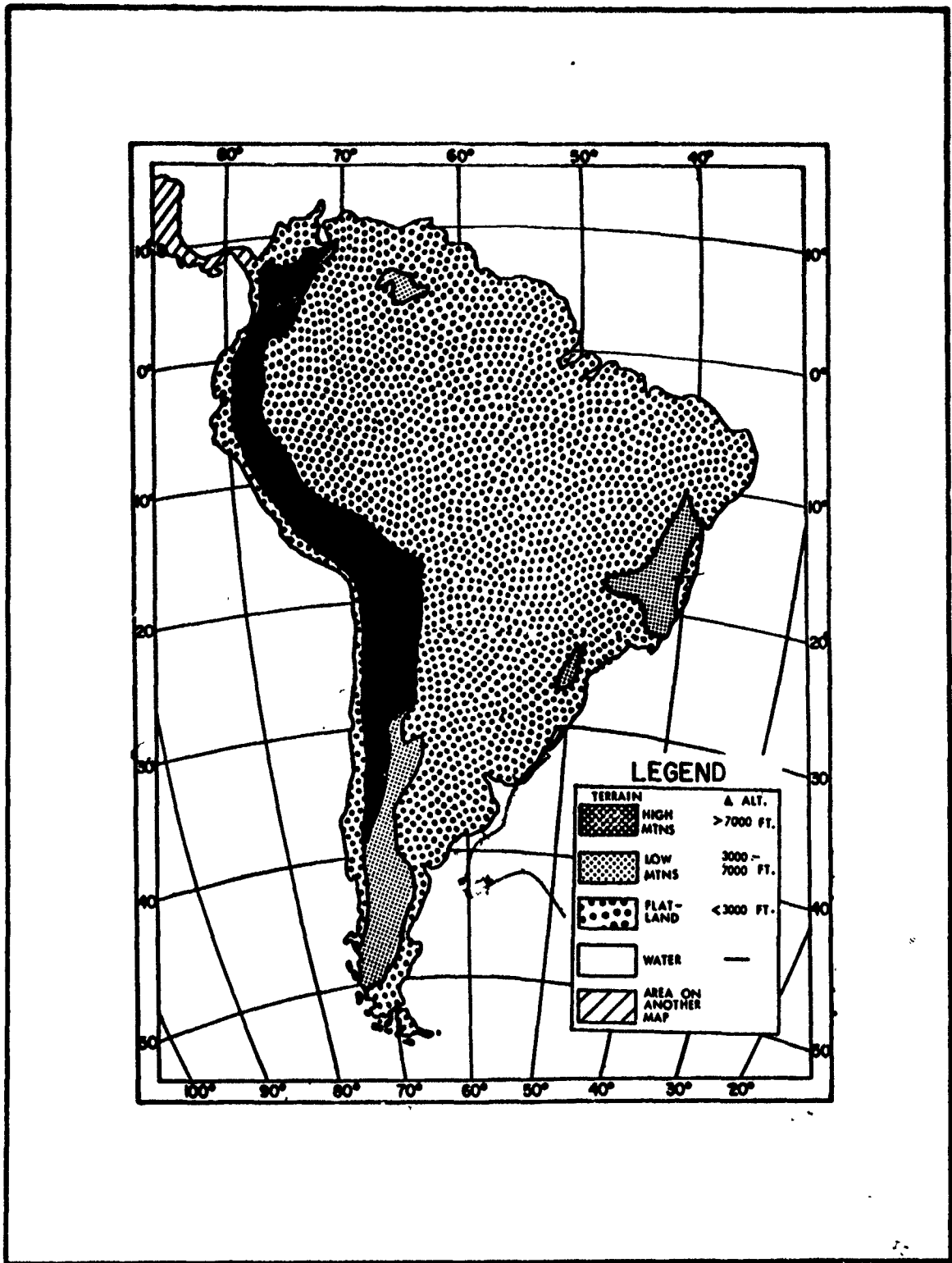


Figure 20. South America - Relief Differences

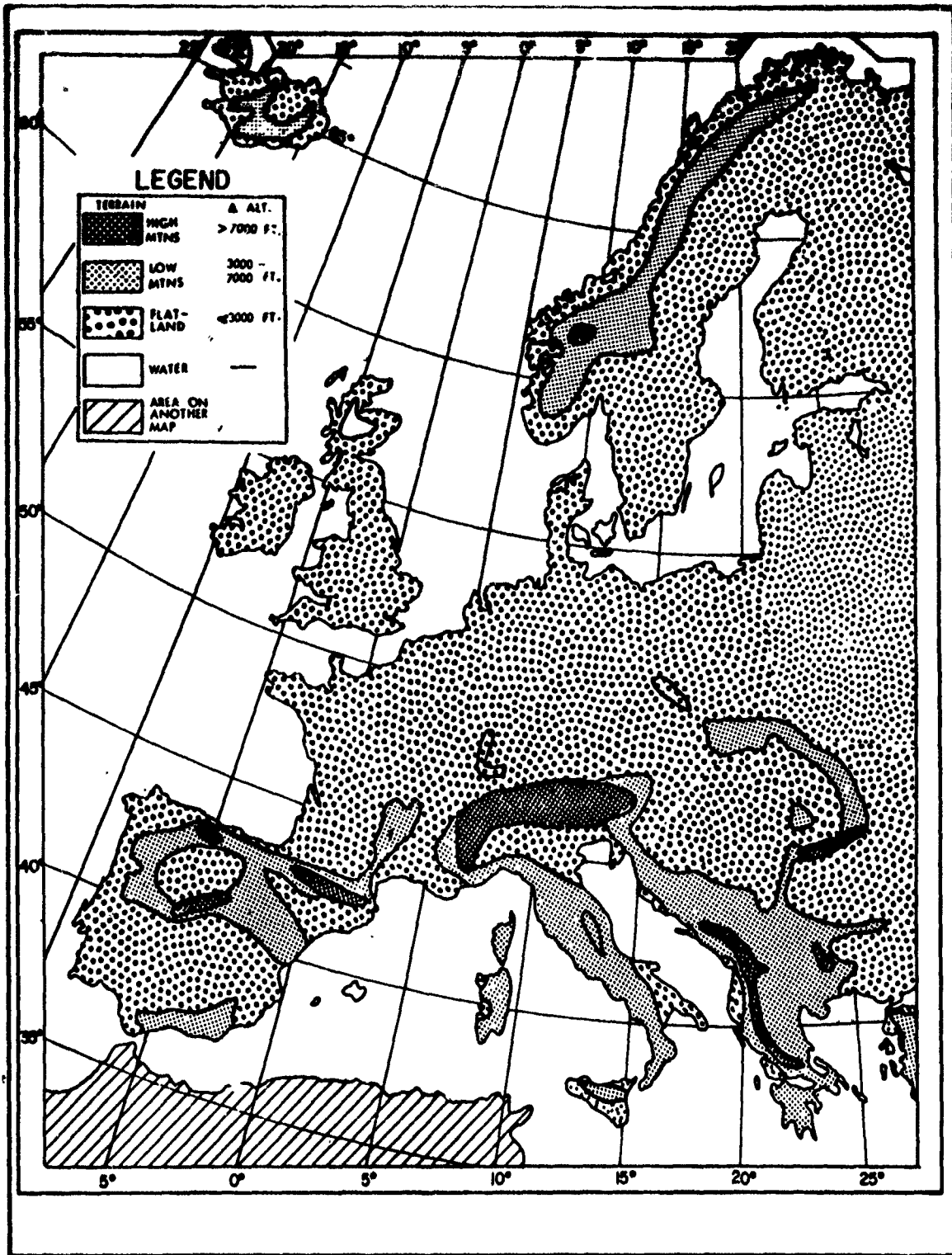


Figure 21. Europe - Relief Differences

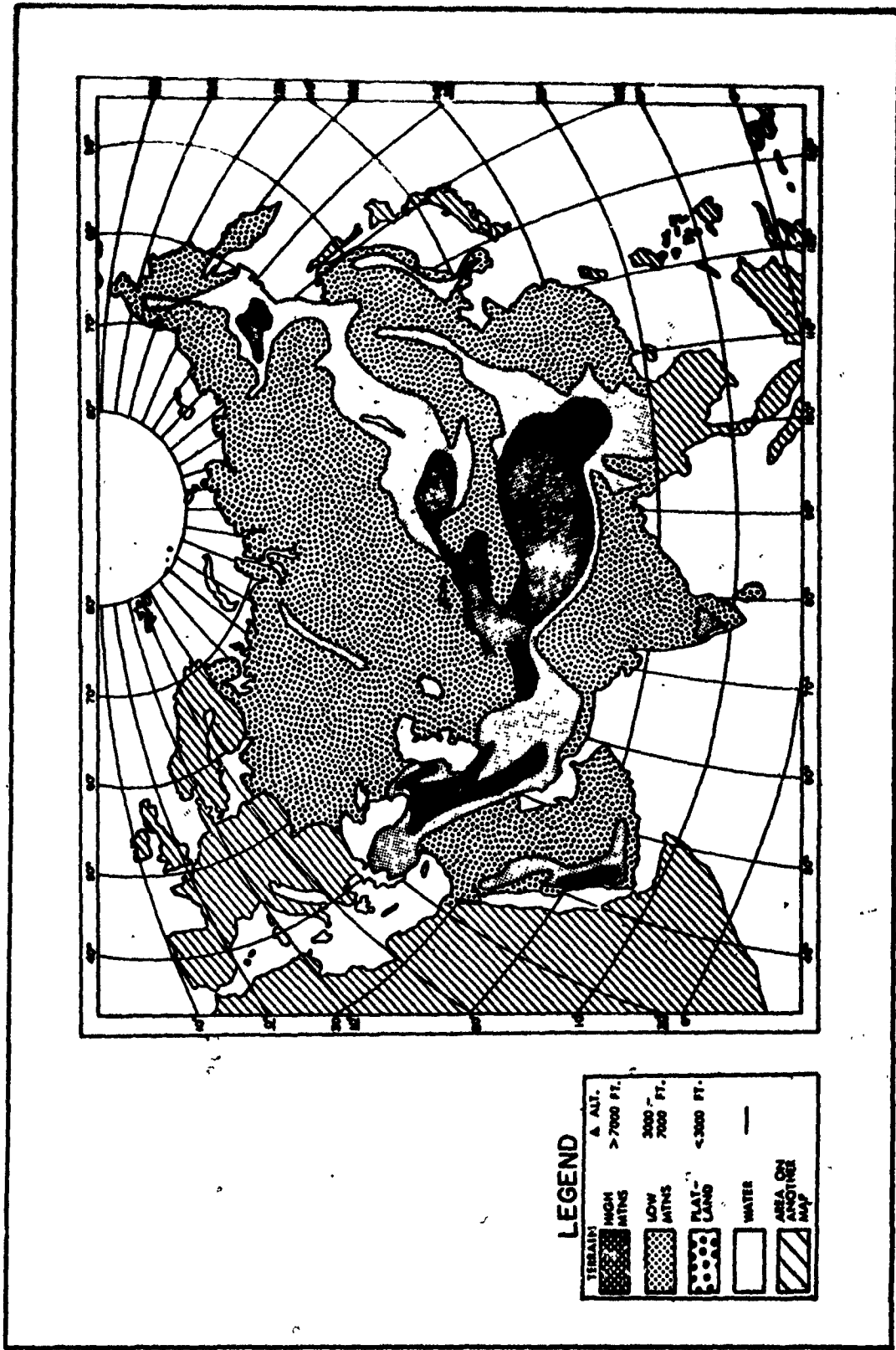


Figure 22. Asia - Relief Differences

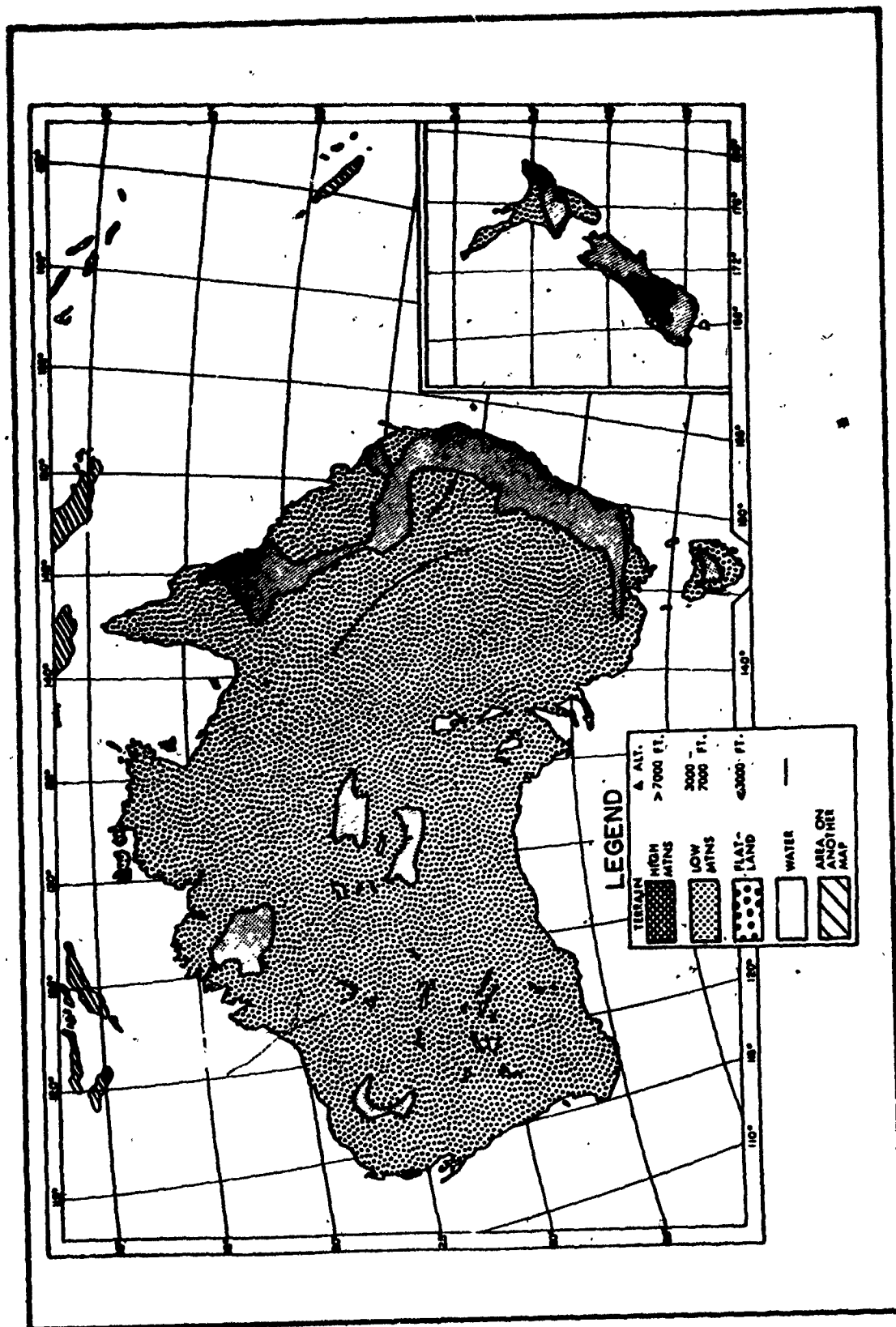


Figure 23. Australia - Relief Differences

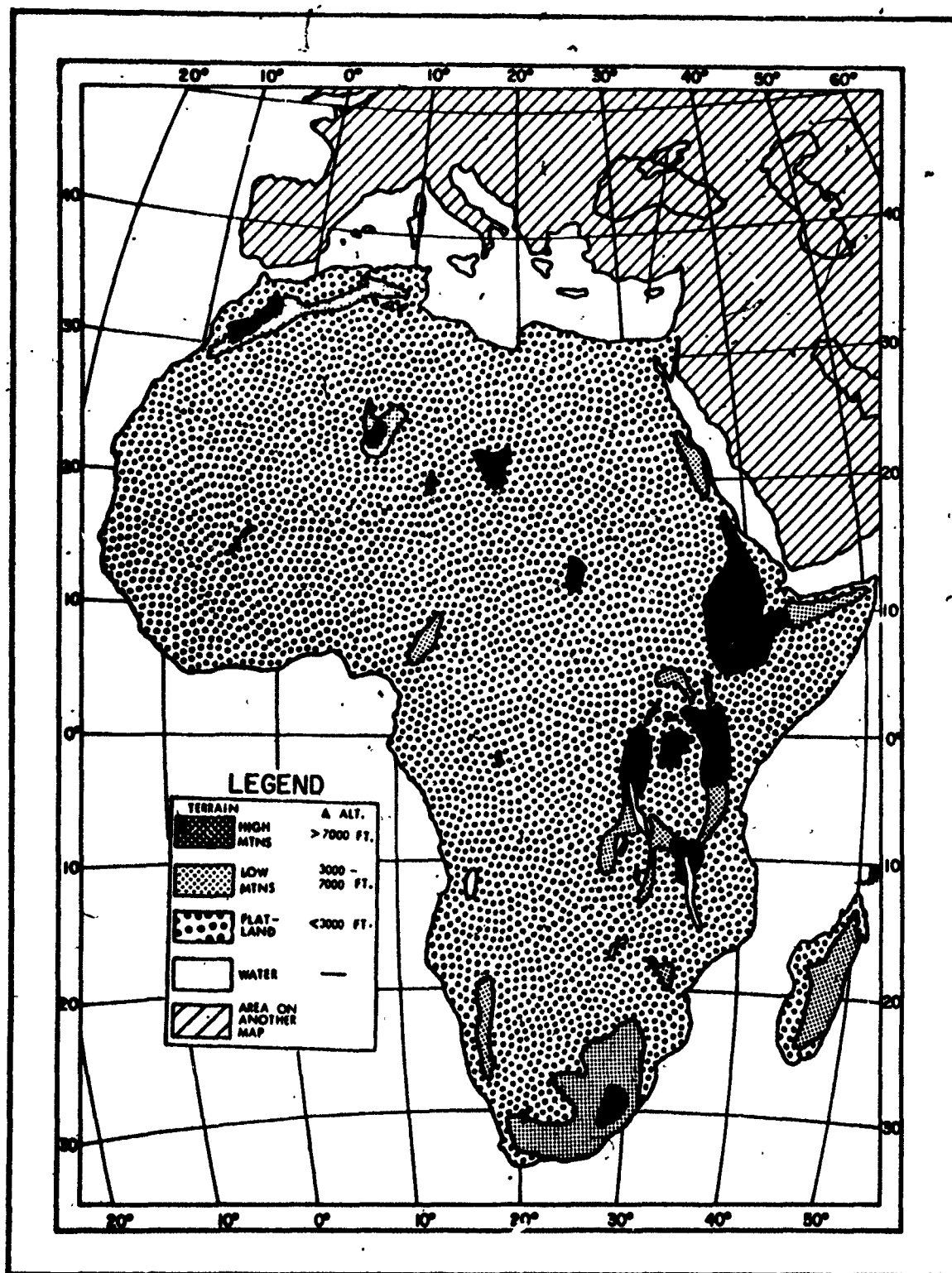


Figure 24. Africa - Relief Differences

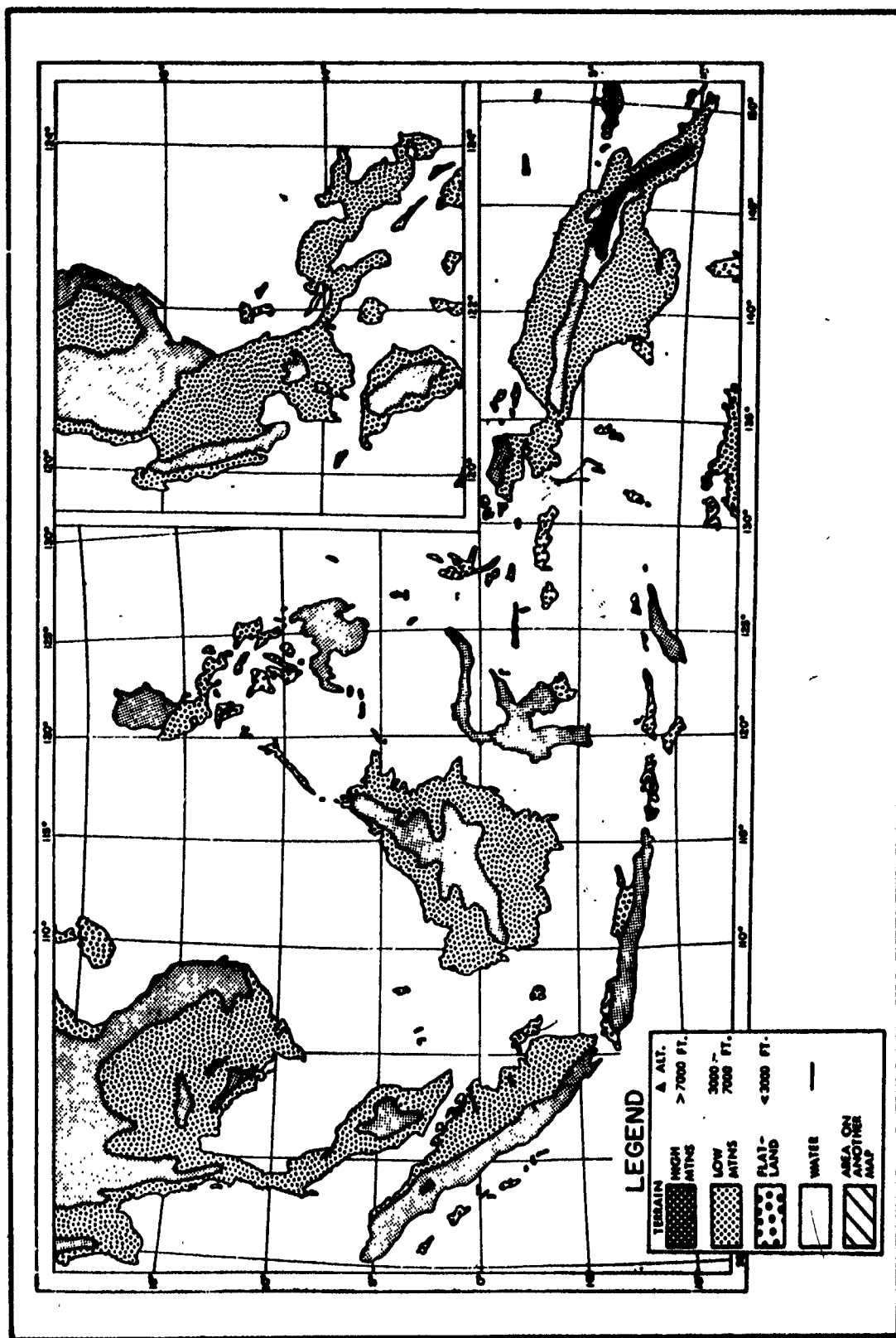
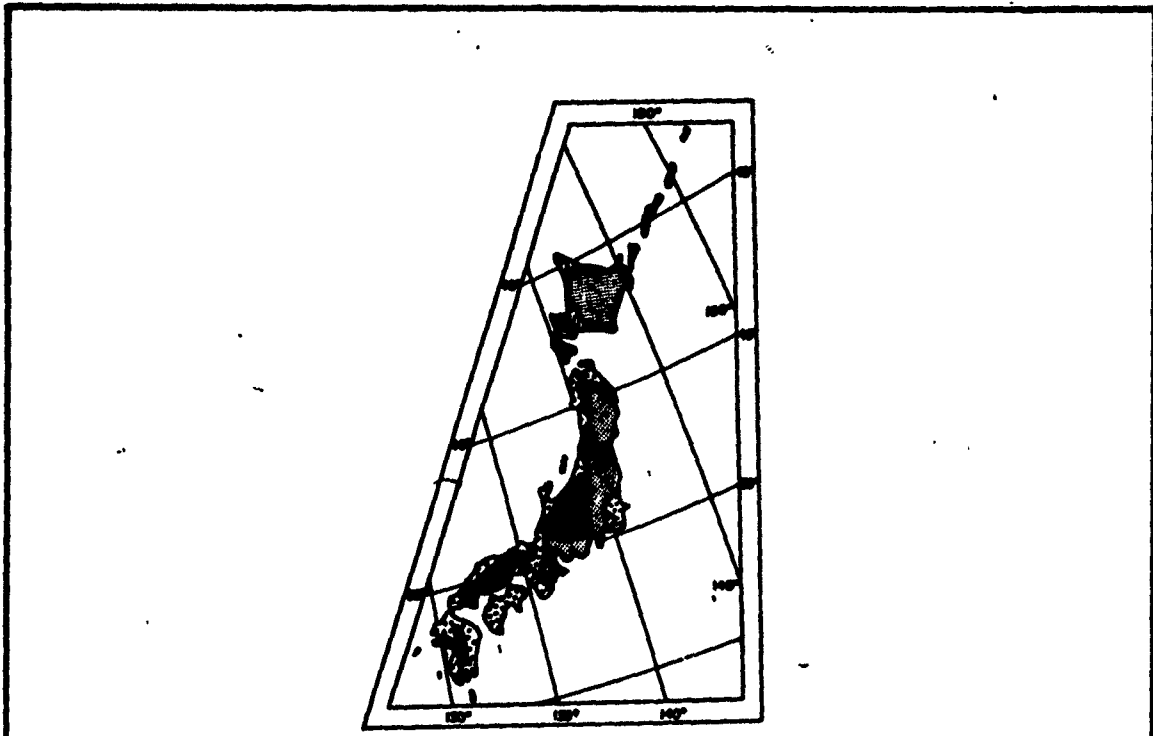
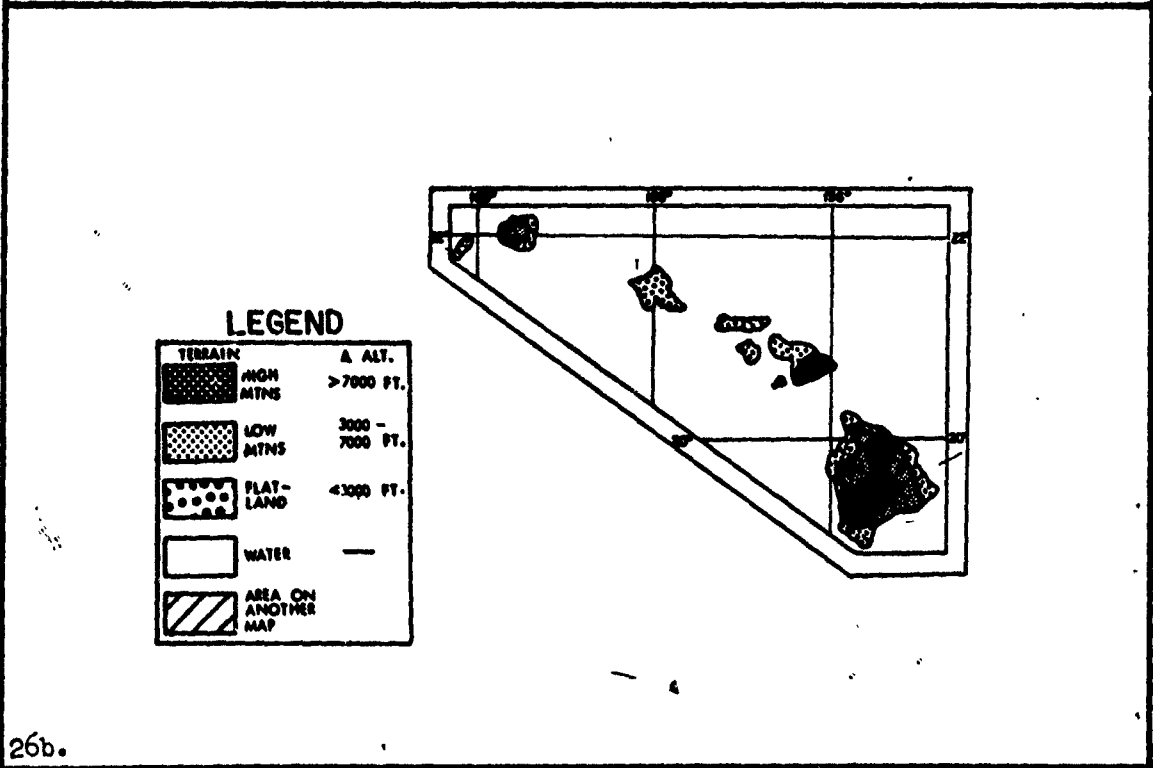


Figure 25. Southeast Asia - Relief Differences





26a.



26b.

Figure 26a. Japan - Relief Differences

Figure 26b. Hawaii - Relief Differences

## SECTION VIII

### FREQUENCY OF OCCURRENCE OF TURBULENCE AS A FUNCTION OF HEADWIND AND TAILWIND

Turbulence has been shown to have occurred more frequently during periods when the aircraft heading was upwind (Ashburn, Waco, and Mitchell, (3)). A further investigation, using only the 264 runs with wind speed  $> 20$  kts, has shown a westerly wind component in 86% of the runs (Figure 27A) and an aircraft heading with a westerly component 61% of the time in turbulence (Figure 27B). These findings would indicate a higher expectancy of turbulence with a heading into the wind. This is shown to be the case in Figure 27C where 62% of the flight time in turbulence coincided with a headwind component. This increased to 67% for turbulence  $\geq$  moderate. The classification of turbulence was based on peaks in the cg acceleration traces (see Section V).

During several flights, the aircraft was flown in a pattern course, encountering turbulence more than once in the same area. There were 184 runs in pattern flights where the wind equalled or exceeded 20 kts. Over 60% of the time in turbulence was again associated with headwind conditions. This indicates that time of day or selection of flight path cannot be used to explain the increased frequency of occurrence of turbulence with a headwind component.

A distinct difference, however, occurs between the percentage of time in turbulence during headwind conditions for the early flights 54 to 179 (67%) and the redirected flights 180 to 285 (53%). Because the uncertainties in deriving winds were greater in the early phase of the HICAT program, it is concluded that the headwind-turbulence relationship may be explained, in part, as a result of errors in the computed winds in the first set of flights.

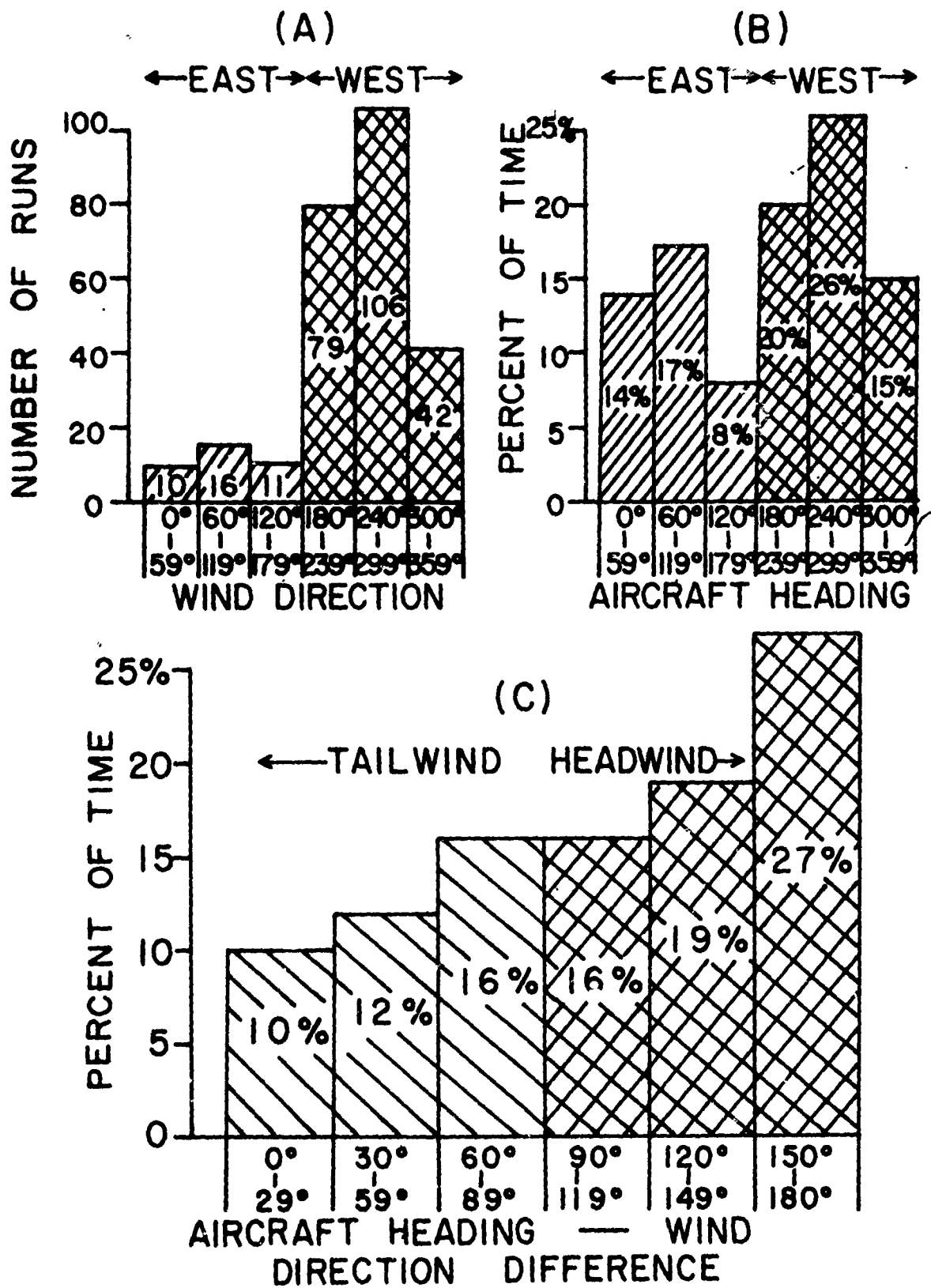


Figure 27A. Frequency of Occurrence of 264 Runs by Wind Direction; 27B Percent of Time in Turbulence by Aircraft Heading; and 27C Percent of Time in Turbulence by Aircraft Heading - Wind Direction Difference.

## SECTION IX

### POWER SPECTRAL DENSITY CURVES AS FUNCTIONS OF AIRCRAFT HEADING WITH RESPECT TO WIND DIRECTION

#### Introduction

Several spectra with long wavelength cutoffs of 10,000 ft ( $10^{-4}$  cycles/ft), normalized by passing them through the same point at the shortest wavelength, were compared for six flights (Figure 28). Of special interest was the heading orientation with respect to wind direction. Each flight contained spectra from runs obtained in pattern flight over the same general area. Sets of two flights are presented for high mountains, low mountains, and flatland topographic categories.

#### High Mountains

(1) Flight 114: Figure 28A shows three spectra from runs east of the Sierra Nevada ridge line. Turbulence was light. Winds recorded at Oakland, California, and Winnemucca, Nevada, were 80 kts from the southwest at 20,000 ft. Runs 10 and 11 were both crosswind and nearly overlapping in space, yet produced spectra with significantly varying slopes for  $\lambda > 2,000$  ft. All three spectra bend upwards with slopes from 1.67 to 2.64 at longer wavelengths compared to slopes all close to 1.50 for  $\lambda < 2,000$  ft.

(2) Flight 280: Figure 28B. The three runs had moderate to severe turbulence, headings nearly parallel to the windflow and a bending upwards (steeper slopes) at  $\lambda > 1,000$  ft. Run 10, the spectrum with the largest RMS (2,000) value, is the least steep of the three. The flight was between the crest of the Rockies and Denver.

#### Low Mountains

Flight 90: Figure 28C. These spectra were computed from data obtained over North Island in New Zealand. Turbulence was light to moderate. As with the previous spectra there is good agreement for  $\lambda < 1,000$  ft but variable slopes at long wavelengths. Again, the spectrum with the highest RMS (2,000), Run 12, has the shallowest slope at long wavelengths. The steepest spectrum (Run 5) has the lowest RMS (2,000).

Flight 102: Figure 28D. These two spectra agree over all wavelengths and represent conditions on the lee side of the Great Dividing Range in southeast Australia. Moderate turbulence was present. Headings appear crosswind in both cases, although aircraft winds were too variable to establish a definite heading-wind orientation. The spectra bend considerably downward beyond  $\lambda = 1,000$  ft, having slopes of 1.36 compared to 1.64 at short wavelengths. A similarity exists between these and the shape of the spectra for Flight 90, Run 12. The runs of Flight 102 and 90, Run 12 were above low mountains (elevation differences  $< 4,000$  ft) whereas the other samples were associated

with mountains having relief differences > 6,000 ft.

Flatland

Flight 107: Figure 28E. Four spectra are reproduced here from data obtained over southeast Australia during light to moderate turbulent conditions. Slopes vary appreciably for  $\lambda > 1,000$  ft. The spectrum from Run 6, with a crosswind component in the heading, behaves similar to Run 8 which had a heading nearly parallel to the wind. In contrast to the mountain samples Run 9, with the highest intensity, has the steepest slope. The spectra from Runs 6 and 8 bend considerably for  $\lambda > 1,000$  ft. with slopes of 1.05 compared to 1.66 for  $\lambda < 1,000$  ft.

Flight 198: Figure 28F. These were from samplings over thunderstorms in the southeast United States. Slopes vary from 1.19 to 1.44 for  $\lambda > 1,000$  ft. and are close to 1.60 at short wavelengths for all spectra. The bending at long wavelengths is similar in magnitude to many of the flatland and low mountain samples. All of Flight 198's spectra were crosswind and fairly high in intensity showing that the variation in shape under similar orientations can be large.

Summary

Spectral shapes for mountain wave samples appear to depend more on turbulence intensity than flight orientation with respect to the wind. Low intensity spectra tend to bend upward at long wavelengths. The low signal to noise ratio at long wavelengths could be a factor in causing the upward bending. The variation in spectral slopes is as great for similar headings as for different headings with respect to wind direction. The shape of flatland spectra also show no correlation between aircraft heading and wind direction. Their slopes vary considerably at long wavelengths and in general are much flatter than the high mountain samples.

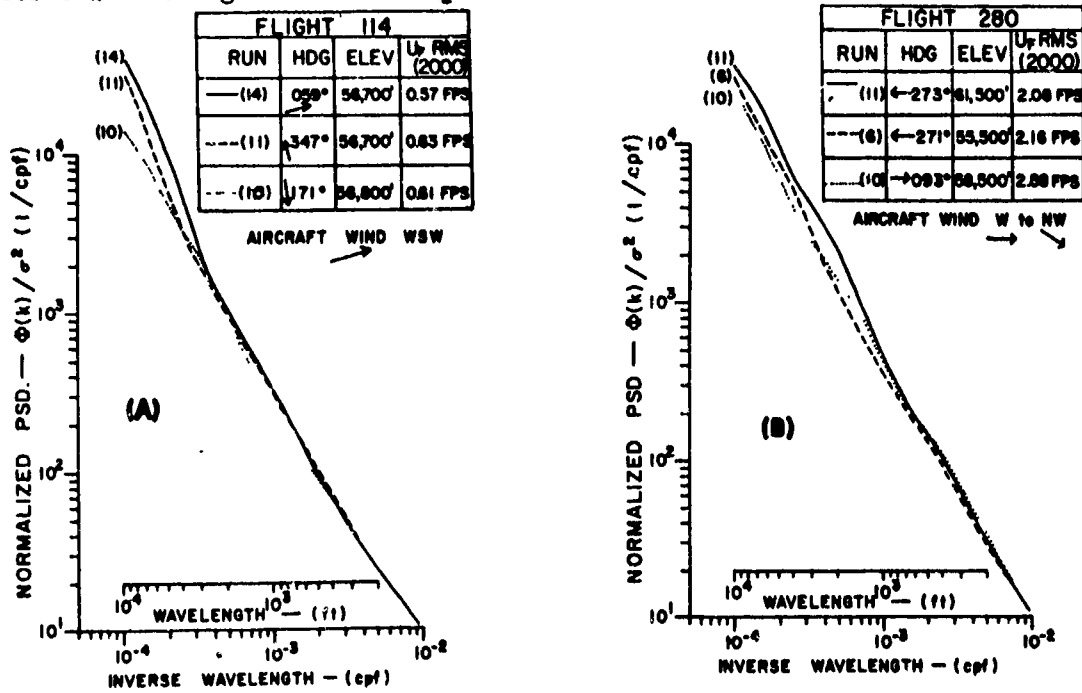


Figure 28A and 28B. Power Spectral Density Curves for Various Aircraft Headings - High Mountains.

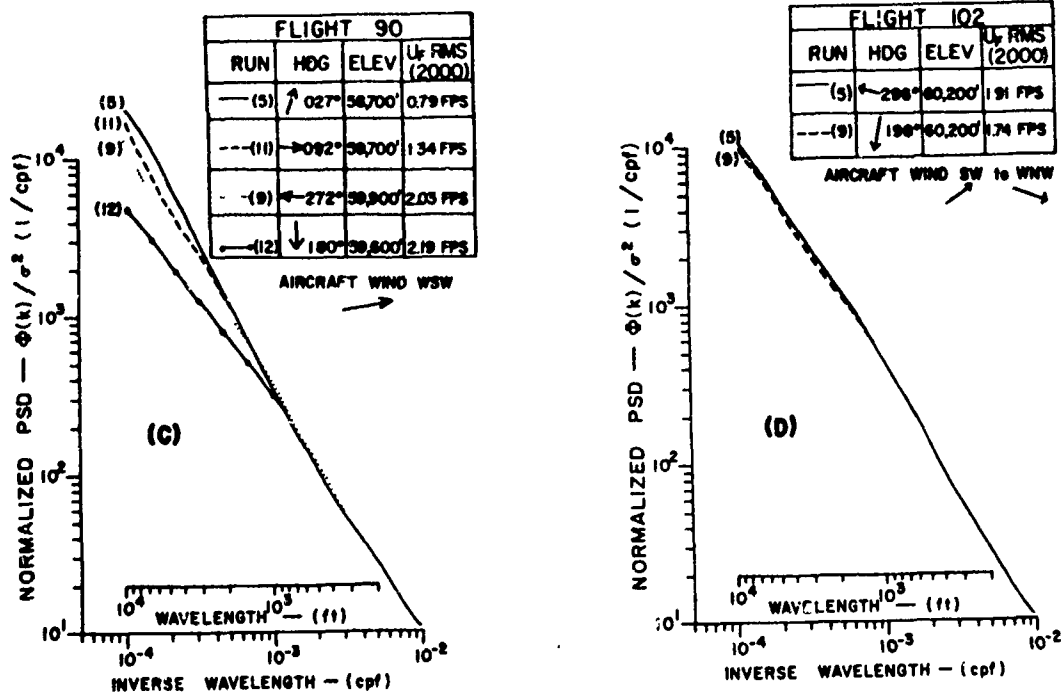


Figure 28C and 28D. Power Spectral Density Curves for Various Aircraft Headings - Low Mountains.

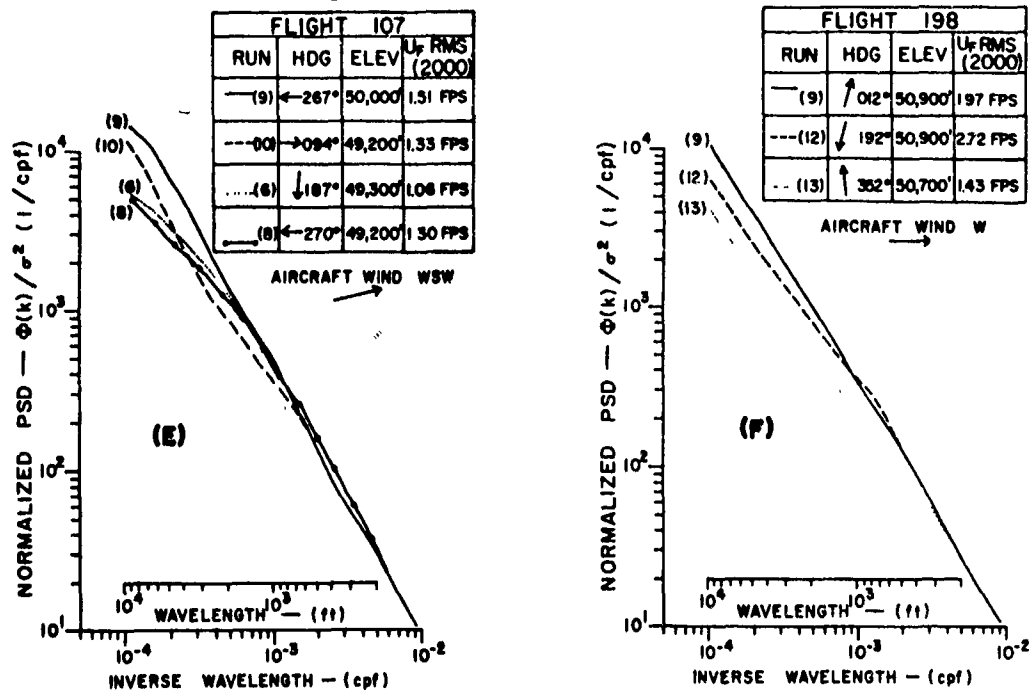


Figure 28E and 28F. Power Spectral Density Curves for Various Aircraft Headings - Flatland.

## SECTION X

### DISTRIBUTION OF TRUE GUST VELOCITIES

#### Introduction

On 15 February 1968 the personnel of the HICAT Project and the National Center for Atmospheric Research cooperated in an investigation of turbulence associated with mountain waves over the eastern Rocky Mountain area near Boulder, Colorado. Four aircraft participated in the experiment. Each aircraft flew a track between Kremling and Akron, Colorado. Each aircraft flew at different altitudes. The HICAT aircraft flew at altitudes of 54,000 to 66,900 ft. For this particular flight the true gust velocities at 0.08 second intervals have been tabulated. Trends were not removed.

#### Distribution of the True Gust Velocities for HICAT Flight 280, Run 11.

Flight 280, Run 11 was made at 61,500 ft. altitude. The heading was  $273^{\circ}$  and the wind was  $276^{\circ}$  at 17 knots (almost a direct head wind). The maximum  $U_{ge}$  values were + 10.5 and -10.3 ft/sec. Root-mean-square gust velocities for the spectra truncated at  $\lambda = 40,000$  ft ( $2.5 \times 10^{-5}$  cycles/ft) are 4.21, 5.22, and 5.48 ft/sec. for the vertical, lateral and longitudinal components, respectively. The corresponding root-mean-square gust velocities obtained from the time histories with trends removed were 4.87, 12.19 and 10.86 ft/sec. The true airspeed was 419 knots and the length of the turbulent period was 539 seconds. A subjective classification of light to moderate was assigned to the turbulence.

Figure 29 illustrates the cumulative frequencies of gust velocities of given magnitudes for each of the three components. Trends were not removed. If the gust velocities were normally distributed the curves would be straight lines. The curves indicate that the gust velocities are not normally distributed and that the turbulence was not isotropic. Computed means are 1.19, 3.65, and - 0.00 ft/sec. for the vertical, lateral and longitudinal components, respectively, and the corresponding standard deviations 4.53, 12.6 and 15.1 ft/sec. The data used to construct Figure 29 are from one sample of turbulence. Analysis of other data is required before broad conclusions may be reached on the distribution of gust velocities.

Crooks et al (2) list the root-mean-square gust velocities computed from the time histories as 4.87, 12.19 and 10.86 ft/sec for the vertical, lateral and longitudinal components, respectively. These are significantly different than the values given above. The difference is associated with data sampling techniques, removal of trends, and the grouping of the data into histograms.

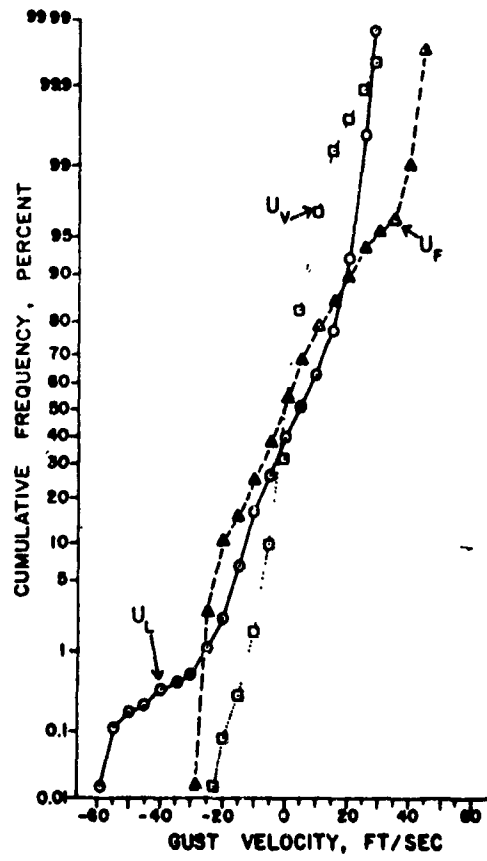


Figure 29. Distribution of True Gust Velocities for Three Components - Flight 280, Run 11.



## SECTION XI

### SUMMARY AND CONCLUSIONS

The principal goal of the analyses presented in this report was to determine numerical values for the standard deviation of the root-mean-square gust velocities ( $b_1$ ), the scale lengths and slopes of the power spectral density curves, and the ratios of turbulent flight miles to total flight miles. These numerical values are given in Tables XIII and XVI. The values of  $b_1$  are shown to increase significantly with roughness of terrain for all three components. Numerical values are 0.9 to 3.4 ft/sec for the vertical component, 1.5 to 4.6 ft/sec for the lateral component and 1.2 to 4.6 ft/sec for the longitudinal component.

There was no well defined trend in the variation of  $b_1$  with altitude. For the total HICAT sample  $b_1$  was equal to 2.3, 3.0 and 3.0 ft/sec for the vertical, lateral and longitudinal components, respectively. The data were inadequate to determine if a further breakdown of each category into "storm" and "non-storm" sets would be useful. The values of the  $b_1$ 's given in this report are dependent, to a large degree, upon the choice of slopes,  $m$ , for the power spectral density curves. When the  $b_1$ 's given in Table XIII are used, it is important to use the appropriate values of  $\bar{x}$  along with the values of  $b_1$ .

Composite spectra were obtained by the use of several techniques, each of which yield different values of  $m$ . None of the techniques indicated consistent slopes of  $-5/3$ . The slopes that are recommended in this report (Table XIII) vary from  $-1.25$  for flights over water to  $-1.55$  for flights over high mountains for the vertical component of the gust velocity. Comparable values for the lateral component are  $-1.50$  and  $-1.75$  and for the longitudinal component are  $-1.45$  and  $-1.60$ . No significant change of  $m$  with altitude was noted. The values of  $m$  for the total HICAT sample are  $-1.45$ ,  $-1.65$  and  $-1.55$  for the vertical, lateral and longitudinal components, respectively. All composite spectra indicated relatively large scale lengths. A scale length of at least 4,000 ft. for all three components is recommended as best fitting the data.

Other conclusions presented in this report may be briefly summarized as follows:

1. The computed values of the  $P'$  but not  $b_1$ 's are significantly affected by the selection of the lower bound of turbulence.
2. The ratio of turbulent to total flight miles was found to be 0.027 for flights over water and flatland, 0.036 for flights over low mountains and 0.049 for flights over high mountains when effects due to pattern flying were removed. These ratios were reduced approximately 35% after examining figures from NASA U-2 programs which contained less bias towards turbulence searching techniques. The overall ratio of turbulent to total flight miles was, in addition, considered to be high because of the larger amount of miles flown over mountains (26%) than

would be expected on a random, world-wide basis (6%).

3. Turbulence decreased substantially with altitude over flat terrain but showed little dropoff with altitude over mountains. Winter appeared to be the season with maximum turbulence.
4. Clear air turbulence existed above thunderstorms at infrequent periods. Therefore, no separate classification was made of turbulence associated with thunderstorm activity.
5. Root-mean-square gust velocities obtained by truncating the spectra at  $\lambda = 2,000$  ft may in most cases be assumed to have a normal probability density distribution, except at large values of the RMS.
6. The probability density distribution of the individual gust velocity values (sampled every 0.08 seconds) has been shown to differ from a normal distribution in one case over mountains.
7. Power spectral density curves for selected cases over various topographic categories showed a wide range of shapes. There was no apparent correlation between spectral shape and orientation of the aircraft with the wind. The mountain wave associated spectra had the steepest slopes with the lower intensity cases showing greater bending upward.

APPENDIX I

DETERMINATION OF SCALE LENGTH BY RMS RATIOS

The equation:

$$\phi(\lambda) = \frac{C}{(1 + 2\pi/\lambda)^{5/3}}$$

when integrated between a truncated  $\lambda$  and the shortest  $\lambda$ , yields the RMS for the truncated  $\lambda$ :

$$\begin{aligned} \text{RMS}(\lambda) &= \left[ \int_{\lambda_a}^{\lambda_b} \phi(\lambda) \right]^{1/2} \\ &= \left\{ \frac{3C}{4\pi L} \left[ \frac{1}{\left(1 + \frac{2\pi L}{\lambda_a}\right)^{2/3}} - \frac{1}{\left(1 + \frac{2\pi L}{\lambda_b}\right)^{2/3}} \right] \right\}^{1/2} \end{aligned}$$

For the HICAT data,  $\lambda_b = 130$  ft.

An expression for the scale length obtained by solving for L in above can be rather involved. Consequently, an alternative method may be used to arrive at L which involves calculating ratios of selected RMS values from the data and equating these to similar ratios obtained from the family of mild knee equations.

$$\frac{\text{RMS}(\lambda_{a_1})}{\text{RMS}(\lambda_{a_2})} = \left[ \frac{\frac{1}{\left(1 + \frac{2\pi L}{\lambda_{a_1}}\right)^{2/3}} - \frac{1}{\left(1 + \frac{2\pi L}{\lambda_b}\right)^{2/3}}}{\frac{1}{\left(1 + \frac{2\pi L}{\lambda_{a_2}}\right)^{2/3}} - \frac{1}{\left(1 + \frac{2\pi L}{\lambda_b}\right)^{2/3}}} \right]^{1/2}$$

where  $\lambda_{a_1}$  was selected as 4,000 ft. or 10,000 ft. and  $\lambda_{a_2}$  as 1,000 ft.

$$\frac{\text{RMS}(\lambda = 10,000 \text{ ft})}{\text{RMS}(\lambda = 1,000 \text{ ft})} = \left[ \frac{\frac{1}{\left(1 + 0.000628L\right)^{2/3}} - \frac{1}{\left(1 + 0.0483L\right)^{2/3}}}{\frac{1}{\left(1 + 0.00628L\right)^{2/3}} - \frac{1}{\left(1 + 0.0483L\right)^{2/3}}} \right]^{1/2}$$

APPENDIX I (Cont)

and

$$\frac{\text{RMS } (\lambda = 4,000 \text{ ft})}{\text{RMS } (\lambda = 1,000 \text{ ft})} = \left[ \frac{\frac{1}{(1 + 0.00157L)^{2/3}} - \frac{1}{(1 + 0.0483L)^{2/3}}}{\frac{1}{(1 + 0.00628L)^{2/3}} - \frac{1}{(1 + 0.0483L)^{2/3}}} \right]^{1/2}$$

#### REFERENCES

1. Crooks, W. M., Hoblit, F. M., Prophet, D. T., et al, "Project HICAT. An Investigation of High Altitude Clear Air Turbulence", Air Force Flight Dynamics Laboratory Technical Report AFFDL-TR-67-123 (Nov. 1967)
2. Crooks, W. M., Hoblit, F. M., Mitchell, F. A., et al, "Project HICAT. High Altitude Clear Air Turbulence Measurements and Meteorological Correlations", Air Force Flight Dynamics Laboratory Technical Report AFFDL-TR-68-127 (Nov. 1968)
3. Ashburn, E. V., Waco, D. E., and Mitchell, F. A., "Development of High Altitude Clear Air Turbulence Models", Air Force Flight Dynamics Laboratory Technical Report AFFDL-TR-69-79 (Nov. 1969)
4. Ashburn, E. V., "Distribution of Lengths of High Altitude Clear Air Turbulent Regions", J. Aircraft 6, 381-2 (1969)
5. Steiner, R., "A Review of NASA High Altitude Clear Air Turbulence Sampling Programs". J. Aircraft 3, 48-52 (1966)
6. Houbolt, J. C., "Gust Design Procedures Based on Power Spectral Techniques", Air Force Flight Dynamics Laboratory Technical Report AFFDL-TR-67-74 (Aug. 1967)
7. Dennis, A., "Lightning Observations from Satellites", NASrO49 (18) Stanford Research Institute, Menlo Park, Calif. (1964) 85 pp.
8. Prophet, D. T., "A Model for Thunderstorm Turbulence", Lockheed-California Company Report LR-23081, (Nov. 1969), 50 pp.
9. Brooks, C., "The Distribution of Thunderstorms Over the Globe", Meteorological Office Geophysical Memoirs No. 24, His Majesty's Stationery Office, London (1925) 20 pp.
10. World Meteorological Organization, "World Distribution of Thunderstorm Days", Part I, TP.6; Part II, TP.21 (1956)
11. "Handbook of Geophysics" (Revised Edition), U.S. Air Force Air Research and Development Command, Air Force Research Division, Geophysics Research Directorate, (The MacMillan Company, New York, 1961) 463 pp.
12. Schonland, B., "Atmospheric Electricity", (John Wiley & Sons, Inc., New York 1953) 95 pp.
13. Long, M., "Tropopause Penetrations by Cumulonimbus Clouds - II", AFCL-65-331, Scientific Report 2, Atmospheric Research and Development Corp., Kansas City, Mo. (1965) 26 pp.

Unclassified  
Security Classification

DOCUMENT CONTROL DATA - R & D

(Security classification of title, body of abstract and indexing annotation must be entered when the overall report is classified)

1. ORIGINATING ACTIVITY (Corporate author) Lockheed-California Company P. O. Box 551 Burbank, California 91503		2a. REPORT SECURITY CLASSIFICATION Unclassified	
		2b. GROUP	
3. REPORT TITLE HIGH ALTITUDE GUST CRITERIA FOR AIRCRAFT DESIGN			
4. DESCRIPTIVE NOTES (Type of report and inclusive dates) Final Report 17 March 1969 to 16 September 1970			
5. AUTHOR(S) (First name, middle initial, last name) Edward V. Ashburn, David E. Waco, Craig A. Melvin			
6. REPORT DATE September 1970		7a. TOTAL NO OF PAGES	7b. NO OF REFS
8a. CONTRACT OR GRANT NO F33615-69-C-1552		8b. ORIGINATOR'S REPORT NUMBER(S) LR-23670	
a. PROJECT NO 682E			
c. 682E-06		8d. OTHER REPORT NO(S) (Any other numbers that may be assigned this report)	
d.			
10. DISTRIBUTION STATEMENT This document is subject to special export controls and each transmittal to foreign governments or foreign nationals may be made only with prior approval of the Air Force Flight Dynamics Laboratory (FDTR), Wright-Patterson AFB, Ohio 45433			
11. SUPPLEMENTARY NOTES		12. SPONSORING MILITARY ACTIVITY Flight Dynamics Laboratory Air Force Systems Command Wright-Patterson Air Force Base, Ohio	
13. ABSTRACT Report consists of analysis of measurements made in HICAT flight program and described in reports issued in 1967 and 1968. Clear air turbulent regions in the altitude range 45,000 to 65,000 ft. varied in length from 1 to 115 nm. Power spectral density curves computed from data from the longer turbulent regions had slopes and scale lengths that varied over a relatively wide range. Composite spectra for altitude and topographic categories for the long turbulent regions had slopes of -1.25 to -1.55 for the vertical component, -1.50 to -1.70 for the lateral component, and -1.45 to -1.60 for the longitudinal component. The scale lengths were all above 8,000 ft. The standard deviations of the root-mean-square gust velocities increase significantly with increase in roughness of underlying terrain. The range in values is 0.9 to 3.4 ft/sec. for the vertical component, 1.5 to 4.6 ft/sec for the lateral component and 1.2 to 4.5 ft/sec. for the longitudinal component. There was relatively little change with altitude. The minimum root-mean-square velocity to be considered turbulence varied 0.95 to 3.02 ft/sec. if truncated spectra were used to establish basic definitions of turbulence.			

DD FORM 1473  
NOV 65

Unclassified  
Security Classification

14 KEY WORDS	LINK A		LINK B		LINK C	
	ROLE	WT	ROLE	WT	ROLE	WT
1. High altitude clear air turbulence						
2. Clear air turbulence						
3. HICAT						
4. Power spectral density curves, altitude, topography, season, slope, scale length.						
5. Probability density distribution three component gust velocity						
6. Proportion of flight miles turbulent, altitude, topography, season.						